ELSEVIER

Contents lists available at ScienceDirect

# Journal of Hydrology

journal homepage: www.elsevier.com/locate/jhydrol



# Research papers

# Historical memory in remotely sensed soil moisture can enhance flash flood modeling for headwater catchments in Germany

Yan Liu<sup>a,\*</sup>, Yong Chang<sup>b</sup>, Ingo Haag<sup>c</sup>, Julia Krumm<sup>c</sup>, Visakh Sivaprasad<sup>a</sup>, Dirk Aigner<sup>c</sup>, Harry Vereecken<sup>a</sup>, Harrie-Jan Hendricks Franssen<sup>a</sup>

- <sup>a</sup> Agrosphere (IBG 3), Forschungszentrum Jülich, 52428 Jülich, Germany
- <sup>b</sup> School of Earth Sciences and Engineering, Hohai University, Nanjing, China
- <sup>c</sup> HYDRON GmbH, Environmental and Hydrological Consulting, Karlsruhe, Germany

#### ARTICLE INFO

#### Keywords: Flash flood Data assimilation SMAP Regression

#### ABSTRACT

The wetness precondition of a catchment affects available soil water storage capacity and infiltration rate, thus influences flash flood generation. Remotely sensed (RS) soil moisture (SM) can provide valuable information on catchment wetness, but typically only represents the top 5 cm of the land surface. However, hydrological models for flash flood simulation need to consider deeper layers to calculate the total soil water storage. Therefore, a key challenge is to link RS SM to total soil water storage and assimilate RS SM into flash flood models to correctly describe initial catchment wetness. In this study, we developed an approach to combine present and antecedent RS SM to infer present soil water storage based on four regression models. The inferred soil water storage from SMAP (soil moisture active passive) SM was assimilated into the operational LARSIM (Large Area Runoff Simulation Model) hydrological model. We tested this new approach with 12 events in the headwater catchments Körsch, Adenauer Bach and Fischbach in Germany. Results show that random forest regression performs the best among the four regression models. The BIC (Bayesian Information Criterion) score suggests that regressions considering antecedent RS SM can well infer soil water storage, resulting in R<sup>2</sup> of 0.85, 0.94 and 0.93 for the Körsch, Adenauer Bach and Fischbach catchments, respectively. Compared to the open loop (without data assimilation) simulations, our approach enhanced the general performance of event simulations with average KGE increases of 0.09, 0.24 and 0.33 for the Körsch, Adenauer Bach and Fischbach, respectively; and the mean error in the 12 simulated event peaks is reduced 15 %. Moreover, the simulation uncertainty is reduced, too. The transferability of the proposed approach to other RS products is also discussed. Although assimilating RS SM can enhance flash flood modeling, it is primarily affected by the uncertainty in precipitation. In the future, the proposed approach should be tested with more catchments and events to verify its general validity.

# 1. Introduction

Studies have shown that the frequency of short-duration extreme rainfall events is increasing on a global scale in response to climate change (Fowler et al., 2021; Guerreiro et al., 2018; Westra et al., 2014). This type of extreme rainfall can induce flash flood events. The term "flash flood" is typically defined as a fast-responding extreme flow of water into normally dry areas triggered by intense rainfall within few hours (Flamig et al., 2020; Saharia et al., 2017). Such events often occur in small catchments with an area of a few hundred square kilometers or less (Zhai et al., 2021). Due to their rapid onset, there is a very limited opportunity and time for an effective response (Hapuarachchi et al.,

2011). As a result, flash floods can cause severe damages to infrastructure and the environment, as well as endanger human lives and livestock. They are among the world's deadliest climate-related natural hazards (Ma et al., 2021; Zhai et al., 2021). It is therefore of great importance to improve flash flood forecasts and reducing associated uncertainties by any means.

As with other hydrological modeling, forecasts and simulations of flash floods are affected by a number of uncertainties. These uncertainties encompass model structure uncertainty (Beven, 1993; Butts et al., 2004; Chang et al., 2023), model parameter uncertainty (Kavetski et al., 2006a; Liu et al., 2022; Schoups and Vrugt, 2010), and errors in meteorological forcing and observations (Bárdossy et al., 2022; Kavetski

E-mail address: yan.liu@fz-juelich.de (Y. Liu).

<sup>\*</sup> Corresponding author.

et al., 2006b; Pianosi and Wagener, 2016; Schalla et al., 2023), e.g., streamflow and soil moisture. In addition to these uncertainties, the initial condition, particularly soil wetness, can significantly impact the generation of floods, including the magnitude and volume of floods, due to the influence of the available soil water storage (Mahdi El Khalki et al., 2020; Nikolopoulos et al., 2011; Tramblay et al., 2012). The implementation of continuous measurements of soil moisture (SM) can facilitate a more accurate quantification of the wetness condition of an area. Consequently, there is potential for improvement in flash flood simulations with SM measurements to determine the initial model conditions prior to the event (Cenci et al., 2017; Crow et al., 2017; Nikolopoulos et al., 2011). In-situ SM measurements can provide accurate SM along the vertical soil profile, however, it is challenging to obtain data across a larger spatial area. With the development of advanced remote-sensing techniques, more remotely sensed soil moisture (RS SM) products are being produced. For example, the Soil moisture Ocean Salinity (SMOS) (Kerr et al., 2012), Soil Moisture Active Passive (SMAP) (Entekhabi et al., 2010), Advanced Scattermeter (ASCAT) (Bartalis et al., 2007), and Advanced Microwave Scanning Radiometer-2 (AMSR-2) (Parinussa et al., 2015) have been launched to provide global-scale SM products. In comparison to other RS products, SMAP has demonstrated superior performance in estimating SM (Chan et al., 2018; Li et al., 2022). Recent research suggested that the integration of RS technologies has the potential to transform soil measurement practices, offering comprehensive, scalable, and cost-effective solutions (Abdulraheem et al., 2023). While they can represent spatial averaged SM at various available spatial resolutions, the disadvantage is that they normally indicate SM of the topsoil layer (top 5 cm) only. It is therefore, crucial to establish the optimal methodology for utilizing RS SM in hydrological simulations, with a view to enhancing flash flood simulations.

Assimilation of RS SM measurements has been widely used to improve the performance of land surface models (De Lannoy and Reichle, 2016; Lievens et al., 2016; Naz et al., 2019). Lievens et al. (2016) demonstrated that the assimilation of RS SM at the catchment scale resulted in enhanced predictive skills. Naz et al. (2019) showed an improvement of SM and runoff simulations at a spatial resolution of 3 km across Europe through assimilating RS SM. For assimilating RS SM observations into land surface models (LSMs), RS SM can be directly linked to simulated SM by LSMs, as LSMs possess multiple vertical soil layers that can correspond to SM measurements at varying depths. In contrast to LSMs, hydrological models are less spatially distributed, comprising sub-catchments, multiple hydrological response units (HRUs), or even a single bucket for the entire catchment. Nevertheless, studies have demonstrated the utility of RS SM observations in enhancing hydrological simulations (Crow and Ryu, 2009; Han et al., 2012; Houser et al., 1998; López López et al., 2016; Pauwels et al., 2001; Pauwels et al, 2020). The major aim of these studies is to improve streamflow simulations at the daily scale. The models applied are less complex in terms of soil representations than the abovementioned land surface models, but still comprise a few soil layers, allowing for direct linkage of RS SM to the top soil layer of a model.

However, there are hydrological models that are widely used or in operation that only consider a single soil layer. Examples of such models include the HBV model (Lindström et al., 1997), Hymod (Wagener et al., 2001), varKarst (Hartmann et al., 2013) and LARSIM (Large Area Runoff Simulation Model, Bremicker, 2000; LEG, 2023). Note that LARSIM will be used in our study as the flash flood model as it is used for operational streamflow and flood predictions in multiple states within Germany. One limitation of this type of models is the inability to link the RS SM of the top soil layer to the entire model soil water storage. The preprocessing of RS SM is a requisite step for data assimilation in models that contain a single soil layer. Few studies have investigated the appropriate usage of RS SM in models with a single soil layer. De Santis et al. (2021) rescaled RS SM to enable their assimilation into hydrological simulations for over 700 catchments in Europe. Laiolo et al.

(2016) employed an alternative rescaling approach to calculate the Soil Water Index (SWI), thereby establishing a link between RS SM and model storage. Nevertheless, how to optimally use RS SM in flash flood simulations is rarely reported, particularly with regard to the hourly temporal resolution. Studies on flash floods currently focus on ensemble simulations to quantify uncertainty (Flamig et al., 2020; Quintero et al., 2012), risk assessment and susceptibility mapping (Arabameri et al., 2020; Ma et al., 2021) and early warning system development (Corral et al., 2019; Zhao et al., 2022). Further investigation is required to improve flash flood predictions using assimilation of RS SM. The core research question is then how information of RS SM time-series can be optimally exploited and linked to model soil water storage in order to improve flash flood model predictions.

In this study, we propose to use present and historical memory of RS SM to infer the present total soil water storage. The historical memory of RS SM is represented by a certain number of antecedent RS SM. These antecedent RS SM (historical memory) in the top soil can travel to deeper soil layers later in time, thus a series of past antecedent RS SM can provide information on the current vertical SM distribution to derive the present total soil water storage. The SMAP SM retrievals were selected as the target RS measurements due to the superior spatial resolution, quality, and accuracy of SMAP in comparison to other RS products. To improve flash flood simulations, we assimilate the inferred soil water storage into the LARSIM model coupled to PDAF (parallel data assimilation framework). We test our approach in three different catchments with four events per catchment (12 events in total). Four regression methods with varying degrees of complexities are assessed to establish a relationship between RS SM and model soil water storage. Furthermore, we demonstrate the transferability of our approach to other RS products. Our work will provide a feasible method to use RS SM measurements of the top soil layer in hydrological models that contain only a single soil layer, with the aim of enhancing flash flood and streamflow forecast.

# 2. Study sites and data

We set the following criteria to select our study sites: 1) hourly forcing and streamflow observations must be available; 2) flash flood events must have occurred in the past 10 years; 3) catchments should be of a relatively small size, considering flash flood occurrence characteristics; and 4) LARSIM model configurations must be available. Finally, three catchments were selected as our test sites: Adenauer Bach, Fischbach and Körsch (Fig. 1). The three catchments were selected to represent two distinct types of systems susceptible to flash floods. Adenauer Bach and Fischbach represent mountainous rural catchments, while Körsch represents an urbanized catchment comprising a considerable proportion of impervious surface areas susceptible to surface runoff generation. Moreover, these three sites allow the testing of our approach in two distinct settings of the LARSIM model, corresponding to different federal states of Germany. All three catchments are composed of basic hydrological response units (HRUs). Each HRU has its own parameters based on soil and land cover information. A group of HRUs constitute irregular sub-catchments for the Adenauer Bach and Fischbach catchments and 1 km  $\times$  1 km regular grids for the Körsch catchment.

The Adenauer Bach catchment is located in the federal state of Rhineland-Palatinate, Germany (Fig. 1). The area of the catchment is 57 km², with the Adenauer Bach river flowing into the Ahr river and finally ending in the river Rhine. The mean streamflow at the Niederadenau gauging station is 0.31 m³/s. The mean annual precipitation (year 2007–2021) is 662 mm/yr, with summer precipitation (June to August) accounting for 34 % of the total annual precipitation at the Nürburg-Barweiler meteorological station. The mean annual temperature is 9.0 °C. The catchment is predominantly covered by forest, accounting for 72 % of the total area. Two rainfall stations close to the catchment are available for the collection of precipitation forcings (Table 1). The streamflow gauge was installed in 2014, and hourly measurements have

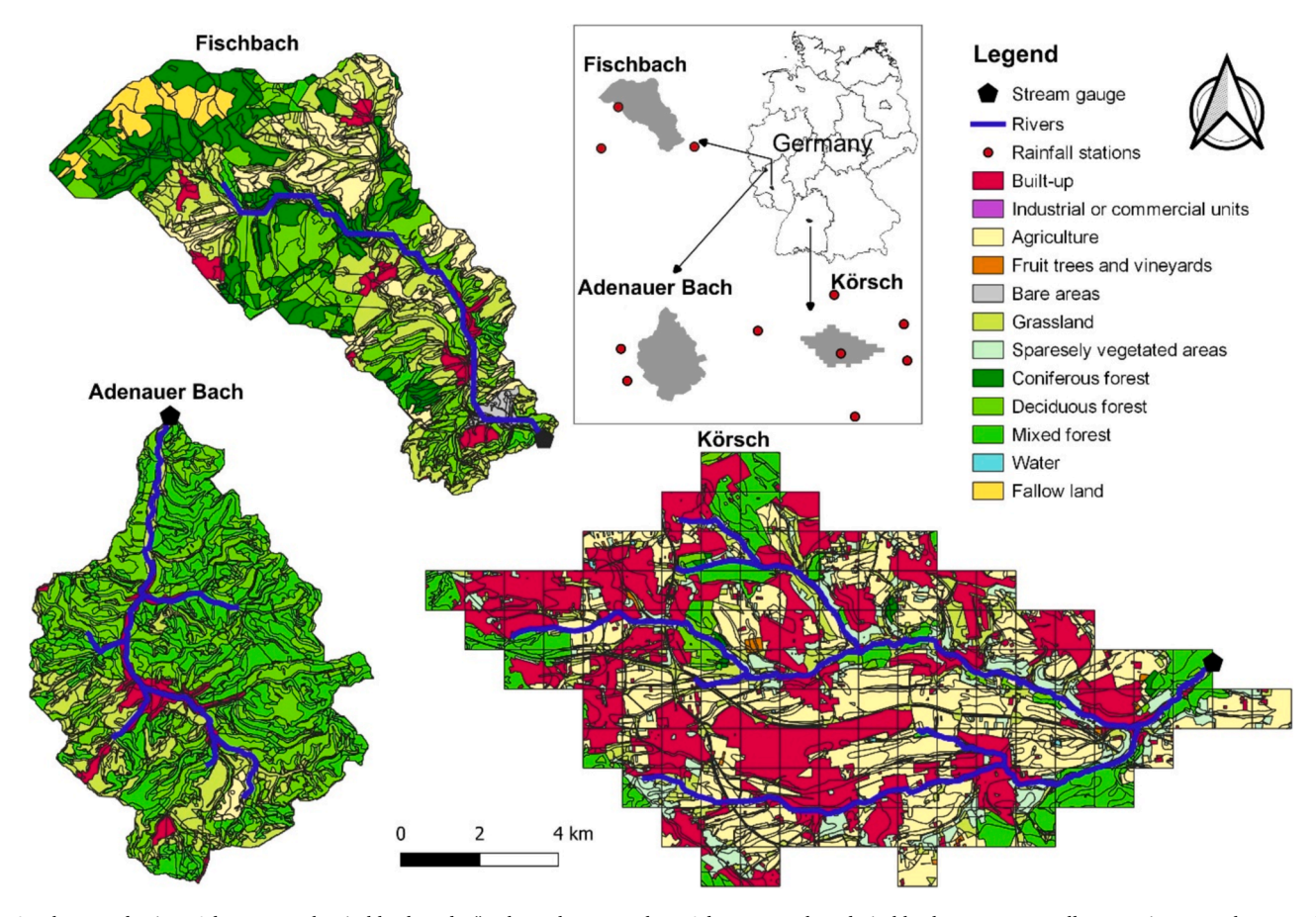


Fig. 1. Three study sites: Adenauer Bach, Fischbach and Körsch catchments, where Adenauer Bach and Fischbach represent small mountainous catchments while Körsch represents a more urbanized catchment. The figure shows the location, rainfall stations, streamflow gauging stations and the distribution of land use types of the three catchments.

**Table 1**Description of forcing datasets, RS SM and streamflow observations.

Category	Data	Temporal resolution	Station IDs of Körsch	Station IDs of Adenauer Bach	Station IDs of Fischbach	Source
Streamflow	Time-series streamflow	Hourly	Denkendorf Körsch (4414)	Niederadenau (2718085500)	Gerach2 (2541075000)	https://udo.lubw.baden-wuerttemberg. de/public/pages/home/index.xhtml https://www.hochwasser.rlp.de/
Forcing <sup>1</sup>	Precipitation	Hourly	00279, 03278, 04160, 04928, 04931, 06275	03660, 04219	0038, 0053, 0360	Deutscher Wetterdienst (DWD) https ://opendata.dwd.de/climate_environment /CDC/observations_germany/climate/h
	Air temperature		04160, 04928, 04931, 06275	03490, 03660	0053, 0360	ourly/
	Air pressure		04928, 04931	03660	2385	
	Global radiation		04928	05100	0053, 0360	
	Relative humidity		04160, 04928, 04931, 06275	03490, 03660	0053, 0360	
	Wind speed		04928, 04931	03660	0053, 0360	
Soil moisture	SMAP (SPL2SMP_E)	Daily	9 km x 9 km			https://nsidc.org/data/spl2smp_e/vers ions/5
	AMSR-2 (LPRM_AMSR2_DS_A_SOILM3)		10 km x 10 km			https://hydro1.gesdisc.eosdis.nasa.gov/d ata/WAOB/LPRM_AMSR2_DS_A_SO ILM3.001/
	ASCAT (ASCAT SSM CDR v7 12.5 km)		12.5 km x 12.5 km			https://navigator.eumetsat.in/prod uct/EO:EUM:DAT:0307
	SMOS (BEC-SMOS-PD-SM-L3v4)		25 km x 25 km			https://bec.icm.csic.es/new-release-of- bec-smos-soil-moisture-products/

<sup>&</sup>lt;sup>1</sup> Meteorological Station IDs: 00279 = Baltmannsweiler-Hohengehren; 03278 = Metzingen; 04160 = Renningen-Ihinger Hof; 04928 = Stuttgart (Schnarrenberg); 04931 = Stuttgart-Echterdingen; 06275 = Notzingen; 03660 = Nürburg-Barweiler; 03490 = Neuenahr, Bad-Ahrweiler; 04219 = Rodder; 05100 = Trier-Petrisberg; 0038 = Bruchweiler; 0053 = Fischbach; 0360 = Leisel; 2385 = Idar-Oberstein.

been recorded since that time. The Fischbach catchment is also located in the federal state of Rhineland-Palatinate, Germany (Fig. 1). It has an area of 63 km<sup>2</sup>, with the river Fischbach flowing into the river Nahe and also ending in the river Rhine. The mean streamflow at the Gerach 2 gauging station is 0.62 m<sup>3</sup>/s. The mean annual precipitation (year 2014–2022) is 665 mm/yr and summer precipitation (June to August) accounts for 27 % of the total annual precipitation at the Fischbach meteorological station. The mean annual temperature is 9.9 °C. Forest covers Fischbach catchment for about 48 % of the total area. Three rainfall stations situated close to the catchment are available to collect precipitation forcing data (Table 1). The Körsch catchment is close to the city of Stuttgart, located in the federal state of Baden-Württemberg, Germany (Fig. 1). Compared to Adenauer Bach and Fischbach, it has a large proportion of built-up areas, ca 34 %, followed by agricultural land accounting for 30 %. The total area of the Körsch catchment is 123 km<sup>2</sup>. with a mean streamflow of 1.31 m<sup>3</sup>/s. The Körsch river flows into the Neckar river which also ends up in the river Rhine. The mean temperature is around 10.5 °C, while the annual mean precipitation (year 2007-2021) is 657 mm/yr with the summer precipitation (June to August) accounting for 38 % of the total precipitation at the Stuttgart-Echterdingen meteorological station. The Körsch catchment has six available precipitation stations including one within the catchment (Table 1). Hourly streamflow has been measured since 1980. Finally, the LARSIM model was configured. The Adenauer Bach and Fischbach catchments were simulated with 49 and 35 irregular sub-catchments (comprising 1985 HRUs and 1825 HRUs), respectively. In contrast, the Körsch catchment was modeled with 123 regular rectangular grid cells (comprising 2434 HRUs).

The hourly meteorological forcing data (Table 1), including precipitation, air temperature, air pressure, global radiation, relative humidity and wind speed, drive the flash flood simulations. They were specifically used to calculate effective precipitation and potential evapotranspiration for the studied catchments. The LARSIM model for the three test sites has been calibrated by the corresponding state agencies according to the guidelines given by Haag et al. (2020). Hourly streamflow

observations were used to compare with event simulations with or without data assimilation. The SMAP SM retrievals were obtained for the sake of data assimilation. Table 1 provides additional details regarding the data.

#### 3. Methods

The true SM at different soil depths can be affected by many factors. e.g., vegetation types and soil characteristics, but is largely influenced by past infiltration events. Soil moisture content is not homogeneous in the vertical direction. However, the LARSIM model, which is used for flash flood simulations, only contains a single soil layer representing the total soil water storage. The RS SM only represents the upper 5 cm of soil, but the antecedent RS SM may provide insights into past infiltration processes in deeper soil layers. Based on this idea, we built the relationship between the current model soil water storage and RS SM considering current and antecedent measurements. The optimal relationship was obtained through the application of several regression models, including linear, polynomial, random forest (RF), and long short-term memory (LSTM) models (Fig. 2). Through that, we inferred current total soil water storage and assimilated it into the coupled LARSIM-PDAF model to improve flash flood simulations. The key components of the framework are illustrated in Fig. 2.

# 3.1. Flash flood model

In this study, we used LARSIM (Large Area Runoff Simulation Model, Bremicker, 2000; LEG, 2023) to simulate flash floods. The reason is that it has been applied in several federal states in Germany and a few other countries for operational purpose, including flood forecasts and hydrological predictions (Bremicker et al, 2013). Therefore, improvements as documented in this work can be incorporated to enhance the operational performance. LARSIM uses irregular sub-catchments or regular (1 km  $\times$  1 km) grids to model the study area of interest. Furthermore, small hydrological response units (HRUs) are used within a sub-catchment or

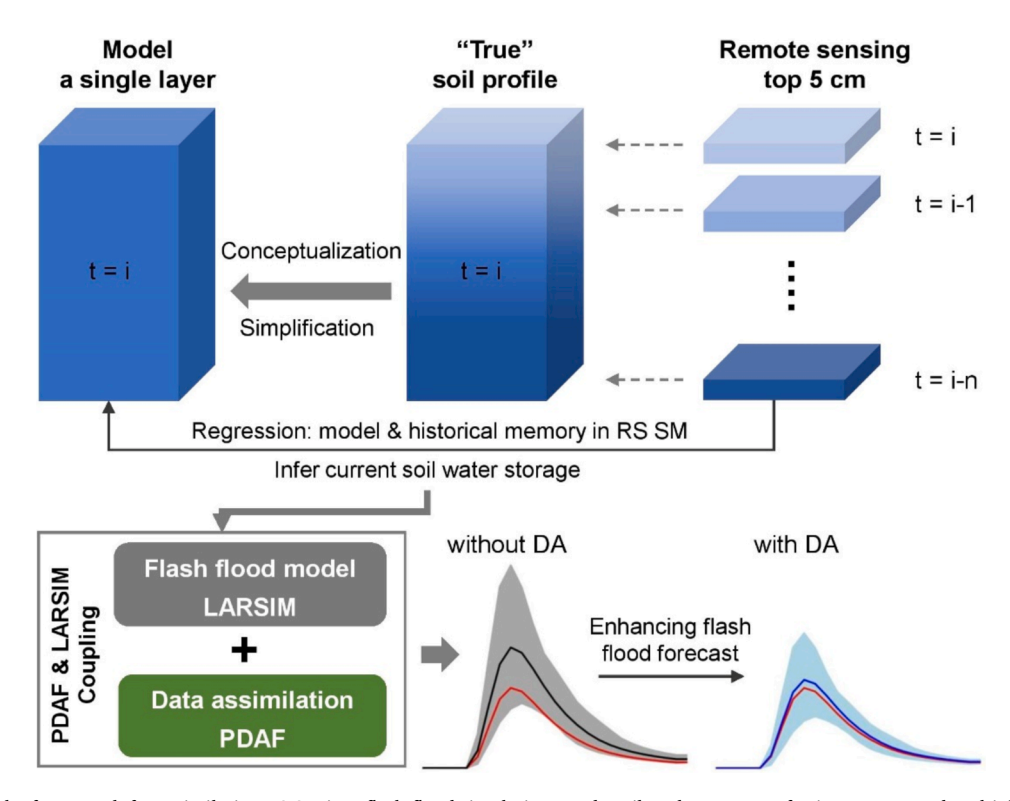


Fig. 2. Schematic of the framework for assimilating RS SM into flash flood simulations. It describes the concept of using current and multiple antecedent RS SM to infer the current total soil water storage and assimilating the total soil water storage in flash flood models.

grid cell, allowing for the consideration of high-resolution spatial information. In this study, LARSIM was executed at an hourly time step for event-based simulations.

LARSIM describes the water balance of a catchment by considering various hydrological processes, including interception, snow accumulation and melting, evapotranspiration, infiltration, soil water storage, runoff generation and channel routing. Since the focus of our study is simulating flash floods, which typically occur in summer months, we focus here on soil water storage and different runoff generation processes. For flash flood simulations, we used a configuration of soil water storage with four runoff components. Furthermore, the dynamic infiltration module, originally developed by Steinbrich et al. (2016) was employed. It accounts for matrix infiltration as well as infiltration via macropores and shrinkage cracks on a physical basis (Haag et al., 2022). Soil water storage is calculated with the water balance equation Eq. (1). The soil-moisture – saturated-areas function Eq. (2) is used to calculate the average saturation of the catchment's area.

$$W_0(t+1) = W_0(t) + P(t) - E_a(t) - QS_{D2}(t) - QS_D(t) - QS_I(t) - QS_B(t)$$
(1)

$$\frac{s}{S} = 1 - \left(1 - \frac{W_0}{W_m}\right)^b \tag{2}$$

where  $W_0(t)$  [mm] denotes the amount of water in the soil storage at the time t; P(t) [mm] is water from precipitation and snow melt;  $E_a(t)$  [mm] is the current evapotranspiration; and the four runoff components are  $QS_{D2}(t)$  [mm],  $QS_D(t)$  [mm],  $QS_D(t)$  [mm] and  $QS_B(t)$  [mm], representing fast direct runoff, slow direct runoff, interflow and baseflow, respectively.  $\frac{s}{s}$  [%] is the portion of saturated areas in the catchment area.  $W_m$  [mm] denotes the maximum soil water storage, and b [-] is a shaping factor.

To calculate the Horton overland flow represented by the fast direct runoff  $QS_{D2}$ , infiltration is simulated on a physical basis, using soil physical parameters and initial soil moisture, and accounting for matrix infiltration as well as infiltration through macropores and shrinkage cracks (Haag et al., 2022):

$$I_{tot} = I_{matrix} + I_{mp} + I_{sc} \tag{3}$$

$$QS_{D2} = \begin{cases} 0, P \le I_{tot} \Delta t \\ P - I_{tot} \Delta t, P > I_{tot} \Delta t \end{cases}$$
(4)

Where  $I_{tot}$  [mm/h],  $I_{matrix}$  [mm/h],  $I_{mp}$  [mm/h] and  $I_{sc}$  [mm/h] represent total infiltration, matrix infiltration, macropore infiltration and infiltration from shrinkage cracks, respectively.  $\Delta t = 1$  h, representing the computational time interval. The other three runoff components are simulated using process-oriented conceptual approaches. Slow direct runoff  $(QS_D)$  is calculated by an explicit soil moisture accounting function (Beven, 2012), where  $QS_D$  increases with increasing soil water storage. Lateral drainage toward interflow  $(QS_I)$  and vertical percolation toward base flow  $(QS_B)$  are generally close to zero for soil water storage below field capacity. Both flows increase exponentially, when field capacity is exceeded and coarser pores are filled with water. The algorithms used for the two different models are described in detail in chapters 3.6.3 and 3.6.7 for Körsch and in chapter 3.6.9 for Adenauer Bach and Fischbach by LEG (2023).

To setup a LARSIM model, physical parameters are derived from digital elevation models and digital maps of soil properties, land cover, and river networks (Bremicker et al., 2013; Haag et al. 2022). There are also conceptual, catchment-specific parameters that are calibrated based on historical observations. Thus, in our study we directly use the calibrated parameters. However, to cover parameter uncertainties for ensemble generations, we consider uncertainties of catchment-specific parameters that are relevant for flash flood simulations. These parameters are described in Tables S1-S3 in the supplement. In our study, LARSIM runs at an hourly resolution, driven by the hourly forcings

described in Table 1, and generates hourly runoff output and soil water storage, which are then used to couple LARSIM with data assimilation.

# 3.2. Regression between RS SM and model soil water storage

#### 3.2.1. Four regression models

To cover a wide range of conditions for building the relationship between model soil water storage and RS SM, we used four different regression models: a widely used linear regression model, a polynomial regression model and machine learning methods including random forest regression and long short-term memory (LSTM). Eq. (5) describes the general form of the regression models. The total soil water storage at t=i ( $S_i[mm]$ ) can be obtained from a function with input variables ( $\theta_i$ ,  $\theta_{i-1}$ ,  $\cdots$ ,  $\theta_{i-p}$ ) and a residual  $\varepsilon_i$  [mm], where  $\theta_i$  [m³/m³],  $\theta_{i-1}$  [m³/m³] and  $\theta_{i-p}$  [m³/m³] denote the RS SM at the present day t=i, one day before i (t=i-1) and p days before i (t=i-p).

$$S_{i} = f(\theta_{i}, \theta_{i-1}, \dots, \theta_{i-p}) + \varepsilon_{i}$$
(5)

Linear and polynomial regressions are described by Eq. (6) and (7). Note that for the polynomial regression, we tested second (k = 2) and third (k = 3) order regressions only to avoid overfitting.

$$S_i = \beta_0 + \beta_1 \theta_i + \beta_2 \theta_{i-1} + \dots + \beta_{n+1} \theta_{i-p} + \varepsilon_i$$
(6)

$$S_i = \beta_0 + \beta_1 \theta_i^k + \beta_2 \theta_{i-1}^k + \dots + \beta_{p+1} \theta_{i-p}^k + \varepsilon_i$$

$$\tag{7}$$

where  $\beta_0$  [-],  $\beta_1$  [-],  $\beta_2$  [-], ..., $\beta_{p+1}$  [-] are the regression constants.

Random forest is a powerful ensemble-based learning algorithm that provides classification and regression (Breiman, 2001) and has been widely used in hydrological studies (Desai and Ouarda, 2021; Liu et al., 2020; Zhang et al., 2018). In this study, we use the regression option to establish the relationship between RS SM and model soil water storage. It builds an ensemble of decision trees trained with the bagging method to make more accurate predictions. The random forest regression is set up in Python using the "RandomForestRegressor" method within the "sklearn.ensemble" package (Pedregosa et al., 2011) using the default value of 100 for the number of trees in the forest.

LSTM is a special type of recurrent neural network (RNN) that can provide a short-term memory for a very long timestep (Hochreiter and Schmidhuber, 1997). It can learn long-term dependencies between input and output variables (Kratzert et al., 2018). Therefore, it could be good for our regression purposes. In this study, three layers in the LSTM were used and the unit number, the dropout rate within these layers, and the learning rate were hyperparameters for tuning. The implementation of the LSTM and the automatic parameter calibration are based on the open-source deep learning library "Keras" (Chollet, 2015).

# 3.2.2. Preprocessing of SMAP SM and model soil water storage

Our aim is to improve flash flood modeling for small catchments ( $\sim\!100~km^2$ ). However, SMAP SM has a spatial resolution of 9 km  $\times$  9 km, which cannot cover detailed SM for small HRUs ( $\sim\!$ few hectares) or model grids ( $\sim\!1~km^2$ ). Due to the problem of the coarse spatial resolution of SMAP SM, the direct comparison of SMAP SM (or regressed SM) to in-situ SM observation is inappropriate given the large spatial heterogeneity. However, we can derive catchment averaged SM based on SMAP and derive "true" catchment averaged soil water storage based on LARSIM simulations considering precipitation uncertainty. The regression is then built between the catchment averaged SMAP soil moisture and catchment averaged model soil water storage.

We use daytime SM retrievals of SMAP, which are from the ascending overpasses. It has missing values, about one in three days. To have continuous data for the regression, linear interpolation is used to fill in these missing values.

A good estimate of soil water storage is crucial for the regression. Uncertainty in precipitation largely affects model simulations of soil

water storage. Therefore, an ensemble of 1000 members was generated to account for precipitation uncertainty. The log-normal multiplicative error model has been broadly used for precipitation perturbation (Crow et al., 2011; Li et al., 2015) and here it was applied to perturb precipitation for all ensemble members. In this study, the mean and standard deviation of the log-normal distribution were set to 1 and 0.25, respectively. Spatial correlations between different meteorological stations are considered, but temporal correlations are not considered in this study. With one ensemble member using the original precipitation, there is a total of 1001 ensemble members. The best 32 performing ensemble members are selected according to the Kling-Gupta efficiency (KGE) for streamflow. Note that these 32 ensemble members are all better than the simulation using original precipitation in terms of streamflow simulations for all catchments. The number of 32 ensemble members is selected to be the same as the number of the ensemble size for later data assimilation. Finally, the mean soil water storage (pseudo observations) of the top 32 simulations is used to build the regression. The model simulation with 32 well-performed ensemble members incorporates precipitation uncertainty both in space and time to a large extent. Therefore, the derived mean soil water storage from these 32 ensemble members can closely represent the "true" catchment averaged soil water storage despite uncertainties arising from unperfect model structure. Given unavailable spatially distributed in-situ SM measurements, the ensemble soil water storage simulations form the semi-independently indirect measurements (the pseudo observations) to validate our regression approach. Despite this limitation, if our regression can match well the pseudo observations, it could capture well the catchment average response.

# 3.2.3. Regression selection

We set up regression models for cases using RS SM considering t=i, from t=i-5 to t=i, from t=i-10 to t=i, ..., and from t=i-180 to t=i. The Bayesian Information Criterion (BIC) is used to determine the optimal number of antecedent days of observations to include in the regression (Laio et al., 2009). As the number of antecedent observations included in the regression increases, the BIC initially decreases, but with continuous increasing of antecedent observations, the BIC begins to increase. The lowest point of the BIC indicates the optimal balance between model fit and complexity. This indicates the optimal number of antecedent days when building the regression. The BIC is calculated by Eq. (8).

$$BIC = -2\ln(L) + k \times \ln(n) \tag{8}$$

where L represents the maximized likelihood of the model, which measures how well the model fits the data. k is the number of independent variables. n is the sample size. In practice,  $-2\ln(L)$  is represented as  $-2\ln(L) = n \times \ln\left(\frac{SSE}{n}\right)$  with SSE the sum of squared errors.

The coefficient of determination  $\mathbb{R}^2$  is also used to measure the goodness of fit of the regression models. Among the four regression models, the one with the highest  $\mathbb{R}^2$  is used to infer soil water storage from SMAP SM.

$$R^{2} = 1 - \frac{\sum_{i=1}^{N} (x_{o}^{i} - x_{m}^{i})^{2})}{\sum_{i=1}^{N} (x_{o}^{i} - \overline{x_{o}})^{2}}$$

$$(9)$$

where  $x_o^i$  and  $x_m^i$  are the *i*-th value of observations and model simulations, respectively.  $\overline{x_o}$  is the mean of observations. N denotes the total number of observations.

# 3.3. Data assimilation

PDAF (parallel data assimilation framework) was selected as the data assimilation tool because it provides many DA methods and supports other useful options such as localization for future development (Nerger

et al., 2005). It also provides a complete and powerful package for coupling with LARSIM. We used the Ensemble Kalman Filter (EnKF) to perform sequential data assimilation.

# 3.3.1. Ensemble Kalman filter (EnKF)

The EnKF (Evensen, 1994) can be described as follows:

$$\mathbf{X}^f = \left(\mathbf{X}_1^f, \mathbf{X}_2^f, \cdots, \mathbf{X}_{nens}^f\right) \tag{10}$$

$$\overline{\mathbf{X}}^f = \frac{1}{nens} \sum_{i=1}^{nens} \mathbf{X}_i^f \tag{11}$$

where  $\mathbf{X}_i^f$  contains the prior model states (before assimilation) for the i-th ensemble member. In this study,  $\mathbf{X}_i^f$  contains the soil water storage of the LARSIM model.  $\overline{\mathbf{X}}^f$  is the ensemble mean and *nens* denotes the ensemble size.

$$\mathbf{P} = \frac{1}{nens-1}\mathbf{X}'\mathbf{X}'^T$$
, with  $\mathbf{X}' = \left(\mathbf{X}_1^f - \overline{\mathbf{X}^f}, \mathbf{X}_2^f - \overline{\mathbf{X}^f}, \cdots, \mathbf{X}_{nens}^f - \overline{\mathbf{X}^f}\right)$  (12).

where  $\boldsymbol{P}$  is the covariance matrix of the model states estimated from ensemble simulations prior to DA updates. The updated soil water storages after assimilation are given by:

$$\mathbf{X}_{i}^{a} = \mathbf{X}_{i}^{f} + \mathbf{K} \left( \mathbf{y}_{i} - \mathbf{H} \mathbf{X}_{i}^{f} \right), \text{ with } \mathbf{K} = \mathbf{P} \mathbf{H}^{T} \left( \mathbf{H} \mathbf{P} \mathbf{H}^{T} + \mathbf{R} \right)^{-1}$$
 (13).

where  $\mathbf{X}_i^a$  contains the updated model states by data assimilation,  $y_i$  is the observation sampled from the distribution with mean equal to the measurement (the soil water storage derived from RS SM based on a suitable regression model) and covariance R. K is the Kalman gain. H represents the observation operator. With the regression approach, we can derive the catchment averaged soil water storage based on RS SM. Using soil water index (SWI, see section 3.3.2), we can derive soil saturation degree and thus calculate catchment averaged soil water storage. The assimilation is based on HRUs to better represent the spatial heterogeneity. The weight of each HRU to the catchment averaged soil water storage is set as the areal fraction (the area of each HRU divided by the total catchment area).

Given the coarse resolution of RS SM, the catchment averaged soil water storage was assimilated. The catchment averaged soil water storage from RS SM was derived using our approach (this is catchment averaged observation), and next the observation operator is applied on the simulation to derive the catchment averaged soil water storage simulation considering the areal fraction of each HRU and the simulated soil water storage for each HRU. With help of the Ensemble Kalman Filter (EnKF), soil water storage of all the HRUs was updated. This allows to find differences in spatially heterogeneous soil saturation of HRUs for open loop runs (no assimilation of RS SM) and data assimilation runs.

# 3.3.2. Ensemble generation and data assimilation settings

Compared to directly using RS SM, the soil water index (SWI) can account for the antecedent soil moisture conditions (Laiolo et al., 2016). In addition to open loop (OL) simulations, we also compare our approach to data assimilation using SWI (DA SWI).

$$SWI_{n} = SWI_{n-1} + K_{n}(SD_{o,n} - SWI_{n-1})$$
(14)

$$K_{n} = \frac{K_{n-1}}{K_{n-1} + e^{-\left(\frac{t_{n} - t_{n-1}}{T}\right)}}$$
(15)

where  $SWI_n$  is the SWI at time step  $t_n$ .  $SD_{o,n}$  represents the observed soil saturation degree at time  $t_n$  in the range [0,1], which is calculated as the RS SM at time  $t_n$  normalized by the maximum RS SM over the entire period.  $K_n$  is the gain at time  $t_n$ , with  $K_1 = 1$  and  $SWI_1 = SD_{o,1}$ . The parameter T characterizes the temporal variation of SM within the rootzone profile and was set to 10 days as suggested by Laiolo et al. (2016). The catchment averaged SWI is calculated and later used for DA.

After testing different ensemble sizes (16, 32, 64, 96, 128), using 32 ensemble members performs well for data assimilation and maintains an efficient computation. Therefore, the ensemble size was 32 in our study. To generate ensemble members, uncertainty in precipitation, model parameters and initial model soil water storage was considered.

As already used in other studies for precipitation perturbation (Han et al., 2014; Strebel et al., 2022), we used the multiplicative log-normal distribution with the mean equal to 1 and the standard deviation equal to 0.25. The temporal correlation is not included but the spatial correlation between different meteorological stations is included in the perturbation.

In addition to the perturbation of the meteorological forcings, catchment model parameters are perturbed as well. A normal distribution is adopted for each parameter with a mean equal to the prior calibrated value and a standard deviation given in Tables S1-S3. If the perturbed values are outside a suggested parameter range, they are set to the corresponding lower or upper limits.

To characterize the uncertainty in the initial model soil water storage, the model is run with calibrated parameters to the time point when data assimilation will be conducted, which is the time with the available SMAP SM just before the event and the catchment averaged initial soil water storage  $S_{ini}$  is calculated. A normal distribution to perturb initial soil water storage is adopted for the initial soil water storage with a mean equal to  $S_{ini}$  and a standard deviation 20 % of the maximum soil water storage capacity  $S_{max}$ . To evaluate different degrees of uncertainty in the initial soil water storage, different perturbations with standard deviations of 10 %, 20 % and 30 % of  $S_{max}$  are tested. Among them, perturbations with standard deviation 20 % of  $S_{max}$  provide a good moderate spread of ensemble simulations. Finally, the perturbed initial soil water storage is constrained to the range of  $[0, S_{max}]$ .

Excluding events with missing precipitation measurements since 2015, we used the four largest events from May to October (since our goal is summer events and to avoid snow influence) for each catchment to test our approach (Table 2). The simulation with 32 ensemble members is run for the flood events to obtain the open loop (OL) simulation, which is the ensemble simulation without data assimilation. For the simulations with data assimilation, the data assimilation is first applied to update the initial soil water storage of each ensemble member and then the simulation of the flood event is performed.

# 3.4. Performance metrics and statistical test

We use the Kling-Gupta efficiency (KGE) to measure the general performance of model simulations (Gupta et al., 2009) and use percent error ( $\epsilon$ ) to denote the simulation error for flood peaks.

$$KGE = 1 - \sqrt{(r-1)^2 + (\alpha-1)^2 + (\beta-1)^2}$$
 (16)

$$\varepsilon = \left| \frac{(X_m - X_o)}{X_o} \right| \times 100\% \tag{17}$$

**Table 2**Simulated events in the Körsch, Adenauer Bach and Fischbach catchments.

Catchment	Date	Peak discharge [m <sup>3</sup> /s]
Körsch	2021-6-28	57.44
	2018-6-7	34.24
	2016-5-30	28.28
	2019-8-7	25.07
Adenauer Bach	2021-7-14	46.86
	2016-6-2	21.99
	2015-9-1	6.46
	2019-10-20	2.33
Fischbach	2018-5-27	59.23
	2018-6-1	13.14
	2016-5-30	6.68
	2021–6-24	5.51

with  $\alpha = \frac{\sigma_m}{\sigma_o}$  and  $\beta = \frac{\mu_m}{\mu_o}$ , where  $(\mu_m, \sigma_m)$  and  $(\mu_o, \sigma_o)$  are the mean and standard deviation of model simulations  $X_m$  and observations  $X_o$ , respectively.

To assess whether improvements of flash flood modeling by the assimilation of RS SM into the LARSIM model is statistically significant, the one-tailed paired Wilcoxon signed-rank test (a non-parametric test) was performed. Based on all 12 simulated events from the three studied catchments, the paired data (OL vs. DA) were prepared. Then the statistical test was carried out for the general event performance KGE, percent error and uncertainty of the simulated events. Here the mean and median of 32 ensemble simulations are used. The event uncertainty is calculated as: (max - min of the ensemble simulations) / observation. The significance level is 0.05.

#### 4. Results

#### 4.1. Performance of regression models

Comparing pairs of observed RS SM and LARSIM soil water storage (Fig. 3a, d and g) in the Körsch, Adenauer Bach and Fischbach catchments, we can see that a specific RS SM can correspond to a wide range of LARSIM modeled soil water storage. This suggests a non-linear and strongly scattered relationship between RS SM and LARSIM soil water storage, indicating that it is not appropriate to use only a single RS SM at a specific date to infer the soil water storage at the same date. Fig. 3b, e and h show the performance of the random forest regression for the three study catchments. As more antecedent RS SM information is included in the regression, R2 increases rapidly, but the increase slows down later as RS SM information is further increased, and finally approaches a stable value. The BIC values suggest that the optimal number of antecedent days of RS SM for the regression is 120, 105 and 105 for the Körsch, Adenauer Bach and Fischbach catchments, respectively. This is also confirmed by the very limited increase in R<sup>2</sup> when using more antecedent days, indicating that using more information than suggested by the BIC does not significantly improve the relationship between RS SM and soil water storage. Fig. 3c, f and i show that after including 120, 105 and 105 antecedent days of RS SM, very good regressions are built for all the catchments. The R<sup>2</sup> values are 0.85, 0.94 and 0.93 for the Körsch, Adenauer Bach and Fischbach catchments, respectively. We also see that when the number of antecedent days exceeds 100, the increase in the regression performance is very small for the three catchments. Therefore, if the BIC analysis is not desired, the number of 100 antecedent days can be used for the regression. Our analysis shows that by considering an appropriate historical memory in RS SM, we can well infer the total soil water storage for the LARSIM model even though RS SM represents only the top 5 cm of soil.

# 4.2. Improvement in flash flood simulations

As the OL and DA simulations use the same model structure and parameter perturbation, the influence of assimilating RS SM to improve the initial soil moisture condition can be verified. Fig. 4 shows that assimilating RS SM based on SWI does not result in a simulated ensemble mean discharge consistently closer to the observations (compared to OL simulation) for the three studied catchments. The simulated ensemble mean by data assimilation using SWI is improved only for three out of 12 events, while the other events show a deteriorated performance compared to OL simulation. Our new approach DA\_RF, using antecedent RS SM based on RF results in simulated discharge being closer to observed discharge for 10 out of 12 events, while the other two events show very similar simulated ensemble mean discharge compared to OL simulation. Uncertainty is reduced as measured by the range of flood peak simulations. In particular, it is greatly reduced for the Adenauer Bach and Fischbach catchments (Fig. 4e - 1). However, even with the improvement by RS SM assimilation, we still have overestimation and

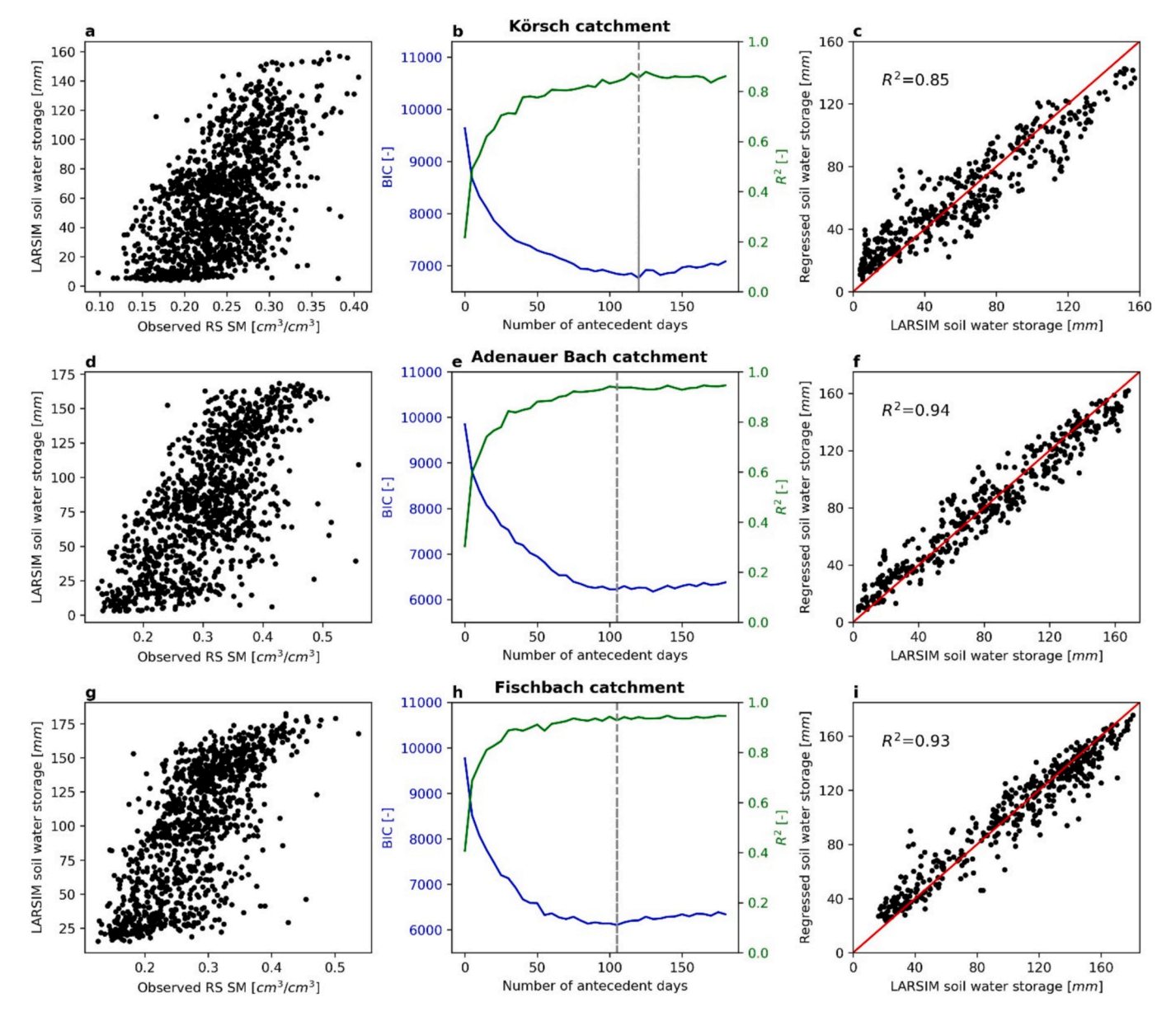


Fig. 3. Relationship between observed RS SM and LARSIM soil water storage (a, d and g), the change in BIC and  $R^2$  (coefficient of determination) with the change in the number of antecedent days considered in the regression model (b, e and h), and the fit of LARSIM soil water storage and regressed soil water storage by RF using RS SM for the case considering 120, 105 and 105 antecedent days (denoted in c, f and i) for the Körsch, Adenauer Bach and Fischbach catchments, respectively. The model soil water storage in this figure is the mean of the 32 best performing ensemble members (see sect. 3.2.2). RF regression outperforms linear regression, polynomial regression and LSTM (see Fig. S1), so only the RF regression is presented here.

underestimation of discharge for some events in the three studied catchments. This indicates that there may be a very large uncertainty in the magnitude and the spatial pattern of precipitation, which largely affects the peak and shape of the flash flood simulation.

Compared to the OL simulations, the DA\_SWI simulations have both improved and deteriorated KGE performance, and this inconsistency indicates some risks by using DA\_SWI to improve flood modeling (Fig. 5). However, compared to the OL simulations, the ensemble members with lower performance were improved by DA\_RF (Fig. 5). Our approach DA\_RF enhanced the general performance with KGE increases of 0.09, 0.24 and 0.33 (average increase of four events per catchment) for the Körsch, Adenauer Bach and Fischbach, respectively (Fig. 5a – c). The ensemble mean error of the simulated flood peaks was reduced by 7%, 18% and 20% (mean reduction of four events per catchment) for the three catchments compared to the OL simulations (Fig. 5e – g). To confirm if the improvement by our approach is statistically significant,

we performed the non-parametric one-tailed paired Wilcoxon signed-rank test (Table 3). We compared the paired ensemble mean and median of 12 events between OL and DA\_RF simulations. It shows that DA\_RF has significantly improved the general performance measured by KGE of the 12 events. The percent error of flood peaks and the uncertainty of flood events of DA\_RF are significantly smaller than that of OL. This indicates the validity of our approach for enhancing flash flood modeling.

Figs. 6, 7 and 8 compare the spatial distribution and uncertainty in soil saturation of the three catchments at the flood peak between OL and DA\_RF. The saturation of each HRU is calculated as the ratio of the HRU-specific simulated soil water storage divided by the HRU-specific maximum soil water storage capacity as derived from model parameters. In general, OL simulated wetter areas than DA\_RF in the Körsch catchment for the event in June of 2021 (Fig. 6). That is why the OL has a larger overestimation of the flood peak than the DA RF for this event in

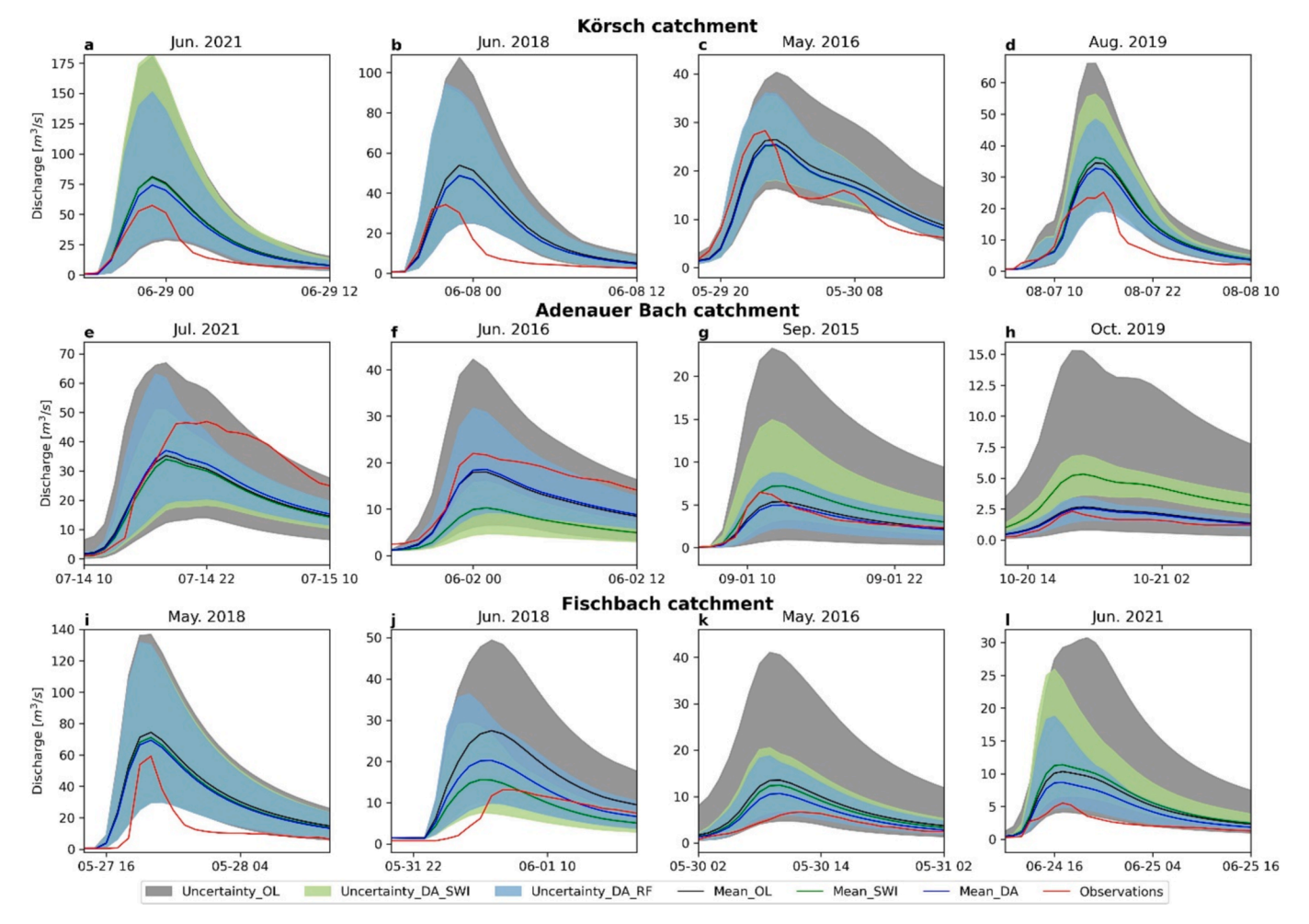


Fig. 4. Comparisons of flash flood event simulations using open loop (OL, without data assimilation), data assimilation using SWI (DA\_SWI), and data assimilation using RS SM based on RF regression (DA\_RF). 12 events were simulated, which are listed in Table 2.

the Körsch catchment. In the Adenauer Bach catchment, both OL and DA\_RF simulate very wet conditions for the example of the event in July 2021, but DA\_RF suggests some wetter areas near the stream, resulting in a smaller underestimation of the flood peak than the OL (Fig. 7). For the event in May 2018 of the Fischbach catchment (Fig. 8), DA\_RF shows generally more drier areas, leading to less overestimation compared to OL. In general, OL has a much larger variance in the soil saturation (Fig. 6d, Fig. 7d and Fig. 8d) than DA\_RF (Fig. 6e, Fig. 7e and Fig. 8e). In particular, the variance of the OL simulations is larger in wet areas. This implicitly suggests that our new approach DA\_RF can reduce the uncertainty in the simulation of spatial soil water storage or saturation.

### 5. Discussion

# 5.1. Historical memory in RS SM is needed for updating present model states

The relationship between the present RS SM and the present model soil water storage (Fig. 3a, d and g) suggests that a single RS SM observation shows only a poor relation with the soil water storage, because RS SM represents only the top 5 cm of soil so that the deeper soil water storage is not well represented. After considering a suitable historical time series of RS SM, we can establish a very good relationship between soil water storage and RS SM. The reason is that the antecedent RS SM can provide information about past infiltration events and thus soil water storage. The number of antecedent RS SM to be included in the regression relationship is in the range of three to four months, which

seems physically plausible. However, the optimal number of antecedent RS SM is different in the three studied catchments (Fig. 3). This is mainly determined by the combined effects of different catchment properties, such as soil type, soil depth and land use, as these factors can strongly influence infiltration processes and water retention in the soil column (Dunne et al., 1991; Thompson et al., 2010). Thus, how many antecedent RS SM should be used is catchment-specific. We also see that the regression is better for the Adenauer Bach and Fischbach catchments than for the Körsch catchment. This could possibly be explained by the fact that the quality of the RS SM is negatively affected by complex topography, surface water and urban structures (El Hajj et al., 2018; Oliva et al., 2012; Wagner et al., 1999). Adenauer Bach and Fischbach are more natural catchments than Körsch, with much less human impacts like, built-up areas. Although the regression analysis suggests that the number of antecedent days is catchment-specific, the improvement in the regression is small when this number is larger than 100. This suggests that in practice if one does not want to run a series of regressions with the BIC criteria, the number of 100 antecedent days can be used for simplification.

The results indicate that RF regression works the best for the selected study sites in this work. However, other regression options could be used in the proposed general framework, based on the performance of different regression models for a specific catchment. De Santis et al. (2021) performed data assimilation of RS SM for over 700 catchments for daily streamflow simulation. They found that on average the improvement by data assimilation is small, especially when soil moisture has reduced control on runoff generation. However they also found

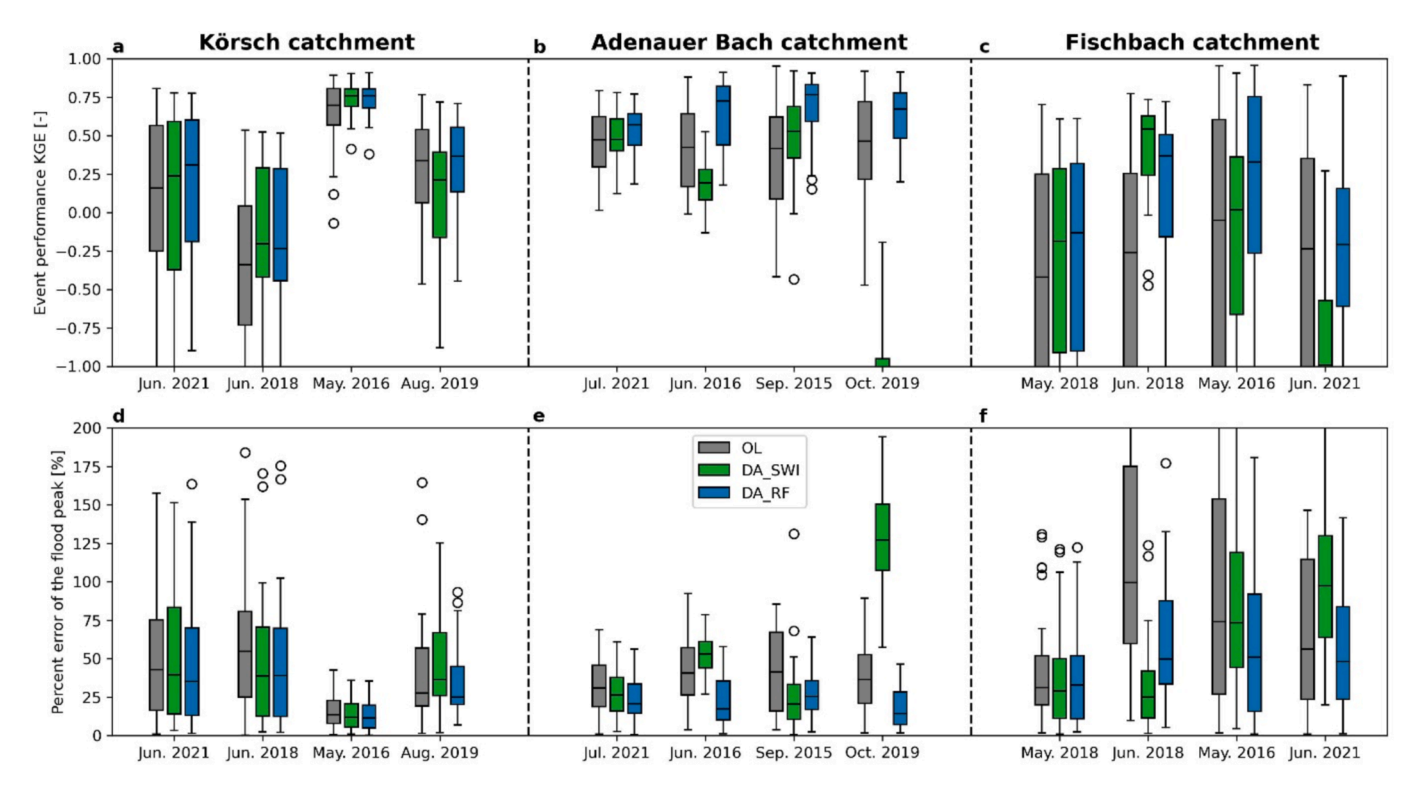


Fig. 5. General performance of flood event simulations (a-c); % error of flood peak simulation (d-f). Results are shown for the open loop (OL, without data assimilation), data assimilation using SWI (DA\_SWI) and data assimilation using RS SM based on RF regression (DA\_RF).

**Table 3**One-tailed paired Wilcoxon signed-rank test based on all 12 simulated events. The significance level is 0.05.

	Hypotheses	P-value	Result
Mean KGE	H0: KGE <sub>DA RF</sub> $\leq$	0.00024	KGE <sub>DA RF</sub> is significantly
Median KGE	$KGE_{OL}$ $H1: KGE_{DA\_RF} > KGE_{OL}$	0.00024	larger than KGE <sub>OL</sub>
Mean percent error	H0: $\varepsilon_{\mathrm{DA\_RF}} \geq \varepsilon_{\mathrm{OL}}$ H1: $\varepsilon_{\mathrm{DA\ RF}} < \varepsilon_{\mathrm{OL}}$	0.00024	$arepsilon_{ m DA\_RF}$ is significantly smaller than $arepsilon_{ m OL}$
Median percent error	$\varepsilon$ : Percent error	0.00049	
Mean event uncertainty	H0: $Unc_{DA\_RF} \ge Unc_{OL}$	0.00024	$Unc_{DA\_RF}$ is significantly smaller than $Unc_{OL}$
Median event uncertainty	$\begin{aligned} &\text{H1: Unc}_{\text{DA\_RF}} < \\ &\text{Unc}_{\text{OL}} \\ &\text{Unc: Uncertainty} \end{aligned}$	0.00024	

*Note*: The subscript DA\_RF and OL represent the option with data assimilation using RS SM based on random forest regression and simulations without data assimilation, respectively.

that larger improvements are observed in catchments with poor OL streamflow predictions and inaccurate precipitation estimates. In our case, the flash flood simulation is at hourly resolution, and the precondition of soil moisture has a very large effect on fast runoff generation. Thus, when the precondition of soil moisture for an event is improved, we see improvements in flash flood modeling. Using antecedent RS SM based on RF resulted in improved flash flood simulations for the three studied catchments, suggesting that considering antecedent RS SM by our proposed approach is a feasible way to appropriately use RS SM to enhance flash flood simulations. Our approach using RS SM to derive the total soil water storage brings three advantages: i) antecedent RS SM (representing upper 5 cm soil) can implicitly represent soil moisture information of deeper soil layers considering travel time from top soil to deep soil, thus combining a certain number of antecedent RS SM can help reconstruct the vertical soil moisture profile given the lack of

vertical soil moisture profile measurements; ii) RS SM used in this approach provides the spatial average soil moisture information of the studied catchment, overcoming the difficulties of using point measurements to derive the catchment averaged wetness condition given a large catchment heterogeneity; and iii) The RS SM data is available in most areas of the world such that the proposed approach may be adapted to different regions easily without additional costs like the installation of soil moisture sensors. Although our approach brings abovementioned advantages, there are few limitations: i) the quality of the regression linking RS SM to total soil water storage strongly depends on the performance of the applied flash flood model in the historical period. The model structure uncertainty and the uncertainty of the historical precipitation measurements can be propagated to the regression, which may lead to bias and uncertainty in deriving the total soil water storage; and ii) although using good ensemble simulations to derive the "true" total soil water storage in the historical period can provide the validation data, it is not an independent dataset, as in-situ measurements would be. However, under real-world conditions very dense in-situ measurement networks are often not available. This leads to a weak validation of our approach. Therefore, in the future testing of our approach at a pilot site with adequate in-situ soil moisture measurements can help to verify its general performance and validity.

Apart from our approach using RS SM to derive initial catchment wetness, using antecedent precipitation might be another alternative. The biggest advantage of using antecedent precipitation to derive catchment wetness is that precipitation measurements are easily available at a high temporal resolution. However, catchment wetness is also largely affected by evapotranspiration. This means that vegetation type and soil property should be accounted for besides further meteorological information (e.g., global radiation). This could make estimating catchment wetness solely from antecedent precipitation challenging. Using RS SM can indirectly account for the influence of evapotranspiration. The antecedent precipitation is also used to help derive catchment wetness prior to a flood event based on the hydrological model. Future work on building relationships between catchment wetness, antecedent

#### Körsch catchment

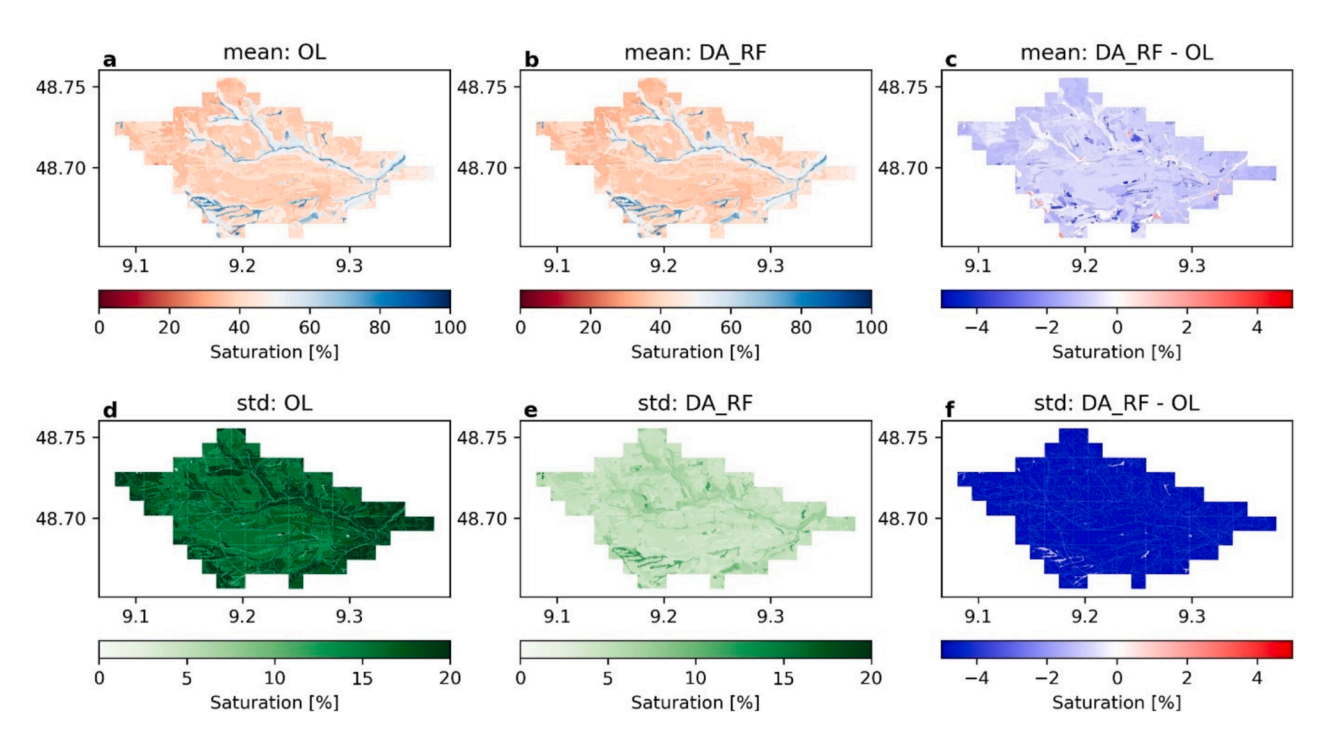


Fig. 6. Comparison of the soil saturation simulation at the flood peak of the event in June 2021 for the Körsch catchment by open loop (OL, without data assimilation) and data assimilation using RS SM based on RF regression (DA\_RF). Since the data assimilation using SWI (DA\_SWI) is not better than OL, here we only present the comparison between OL and DA\_RF for easier visualization.

precipitation and the spatiotemporal distribution of modeled soil water storage may provide some feasible solutions for easier derivation of catchment wetness.

Data assimilation with RS SM can improve modeling, but looking at the peak and extent of flood events the precipitation uncertainty still dominates the total uncertainty. Douinot et al. (2016) showed that the spatial variability of rainfall has a large impact on the catchment response for flash flood forecasting. Yatheendradas et al. (2008) showed that the uncertainty due to depth/volume bias in the radar rainfall estimates almost completely dominated the uncertainty of their flash flood modeling. Therefore, efforts to improve precipitation estimation in both space and time are important and needed to further enhance flash flood simulations. In addition, decomposing the contributions of different factors, e.g., model forcings like precipitation, model parameters and initial conditions, to flash flood simulations would help to identify the relative importance of different factors. For example, using a variancebased approach Thomas Steven Savage et al (2016) could rank the influencing factors for the flood propagation in rivers. Therefore, this kind of analysis can guide us to focus on reducing the uncertainties of the dominant factors.

# 5.2. Transferability of the proposed framework to other RS products

Although SMAP outperforms other RS products (Chan et al., 2018; Li et al., 2022), it has only been available since April 2015. Other RS products may have lower quality but can provide SM for a longer period of time, e.g. AMSR-2 since 2012, ASCAT since 2007, and SMOS since 2010. If our framework can be transferred to these RS products, it may allow the investigation of more historical flash flood events. Compared to SMAP, these products show differences in the spatial resolution (Table 1), data gaps, and the techniques for deriving SM. Therefore, the performance of the transferability should be examined before using these RS products.

We tested RF regression models using AMSR-2, ASCAT and SMOS for the three study sites (Fig. 9), using the same antecedent days as for SMAP. It can be seen that the three RS products all perform better in the Adenauer Bach and Fischbach catchments than in the Körsch catchment, confirming that catchment properties can influence the regression. In general, SMOS performs best among the three RS products, followed by ASCAT and AMSR-2. Looking more closely at the regressions, AMSR-2 shows a larger spread than other products, especially in the Körsch and Fischbach catchments, indicating that it might not be suitable for transferring our framework. The R<sup>2</sup> of SMOS reaches 0.88 and 0.90 for the Adenauer Bach and Fischbach catchments, respectively, and the spread is small, suggesting that the framework can be transferred to SMOS. For ASCAT, the R<sup>2</sup> is slightly lower and the spread is slightly larger than for SMOS, but it still shows the possibility of transferring the framework. Nevertheless, the uncertainty and performance should be verified for specific study areas before transferring the framework to different RS products.

# 6. Conclusions

In this study, we developed a new approach using present and past remotely sensed soil moisture (RS SM) and regression models to better characterize antecedent soil water storage in flash flood simulations. Our approach solves the problem that RS SM cannot be directly assimilated into flash flood models because RS SM only contains soil moisture information for the top 5 cm of soil, while the flash flood model we used (LARSIM) represents the entire soil water storage with a single soil layer. RS SM from SMAP was used to build the relationship between RS SM and model soil water storage based on four regression models. In order to enhance flash flood modeling, the LARSIM model, which is used by several German federal states for hydrological forecasting, was coupled to PDAF, a data assimilation framework, to assimilate RS SM. This new approach was tested for the urbanized Körsch catchment and the

# **Adenauer Bach catchment**

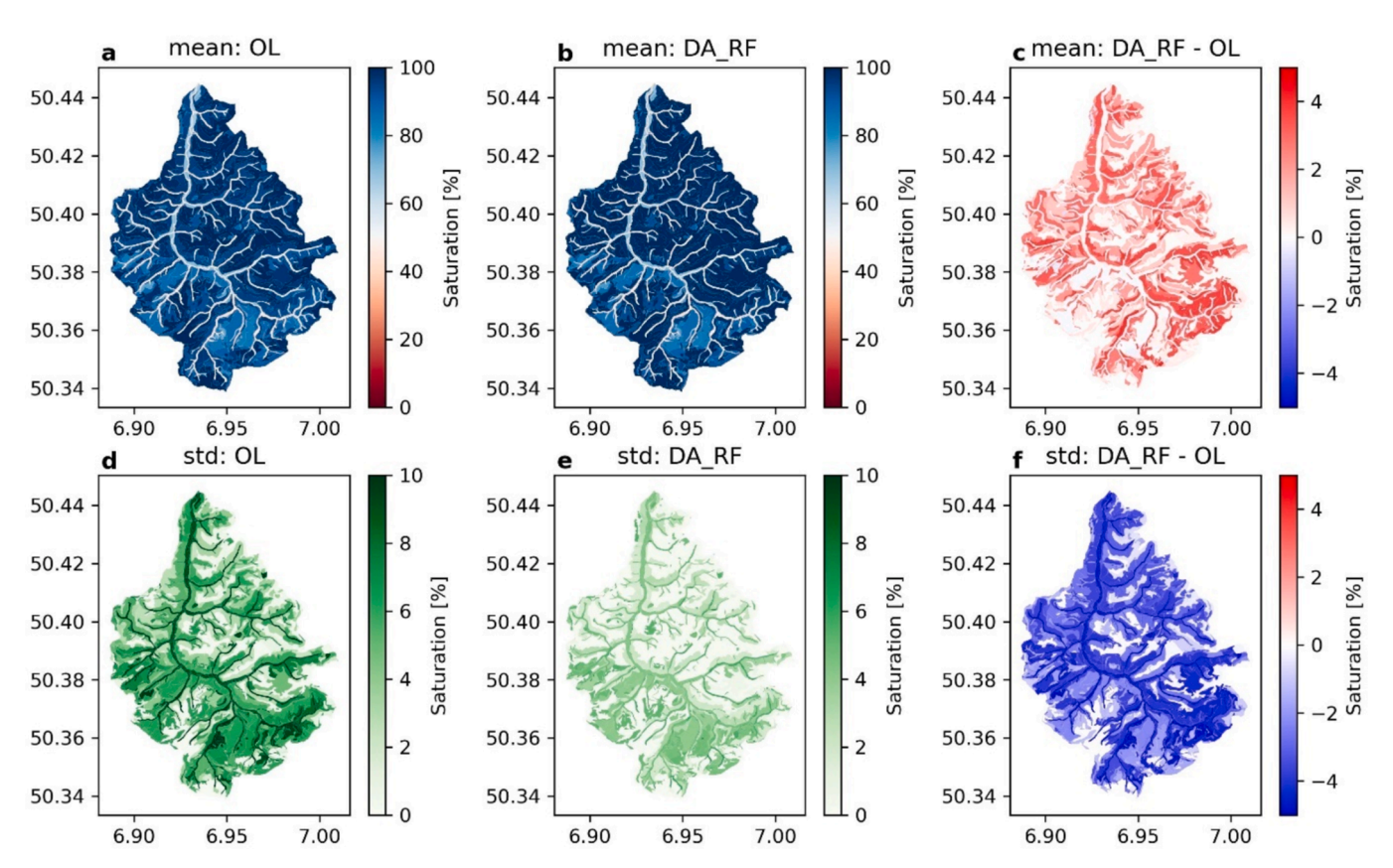


Fig. 7. Comparison of the soil saturation simulation at the flood peak of the event in July 2021 for the Adenauer Bach catchment by open loop (OL, without data assimilation) and data assimilation using RS SM based on RF regression (DA\_RF). Since data assimilation using SWI (DA\_SWI) is not better than OL, here we only provide the comparison between OL and DA\_RF for easier visualization.

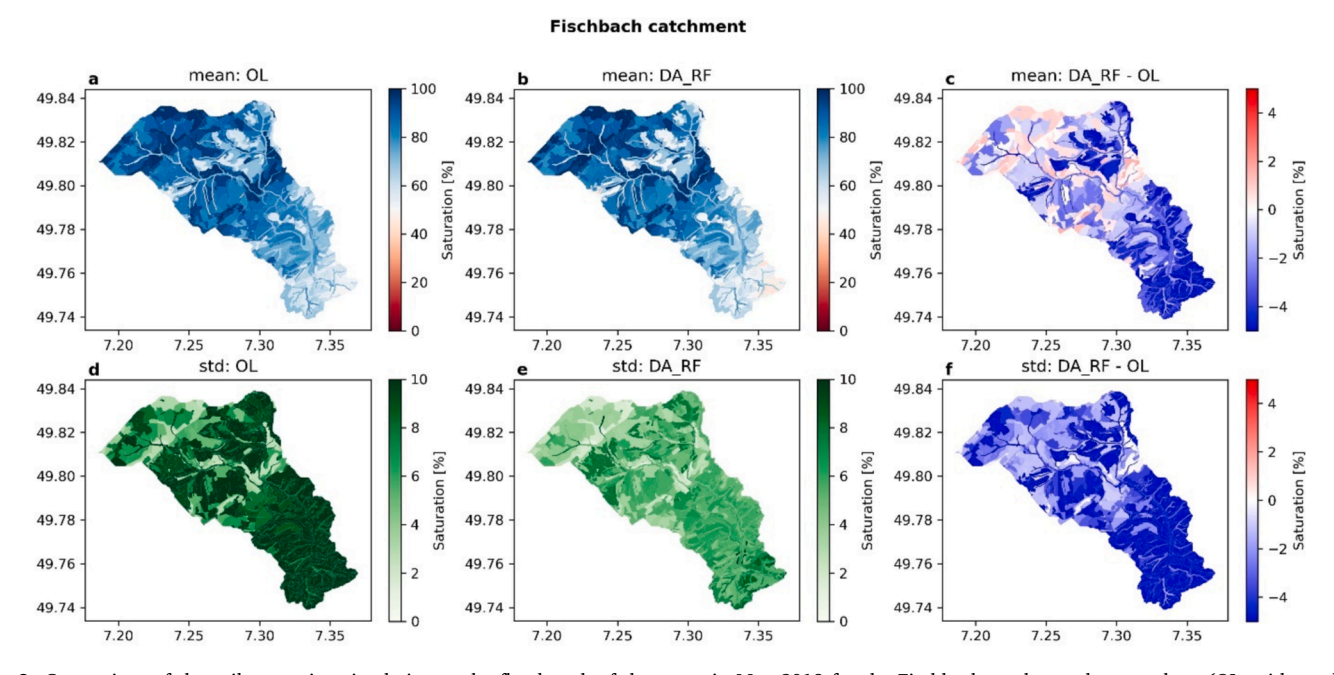


Fig. 8. Comparison of the soil saturation simulation at the flood peak of the event in May 2018 for the Fischbach catchment by open loop (OL, without data assimilation) and data assimilation using RS SM based on RF regression (DA\_RF). Since data assimilation using SWI (DA\_SWI) is not better than OL, here we only provide the comparison between OL and DA\_RF for easier visualization.

Y. Liu et al.

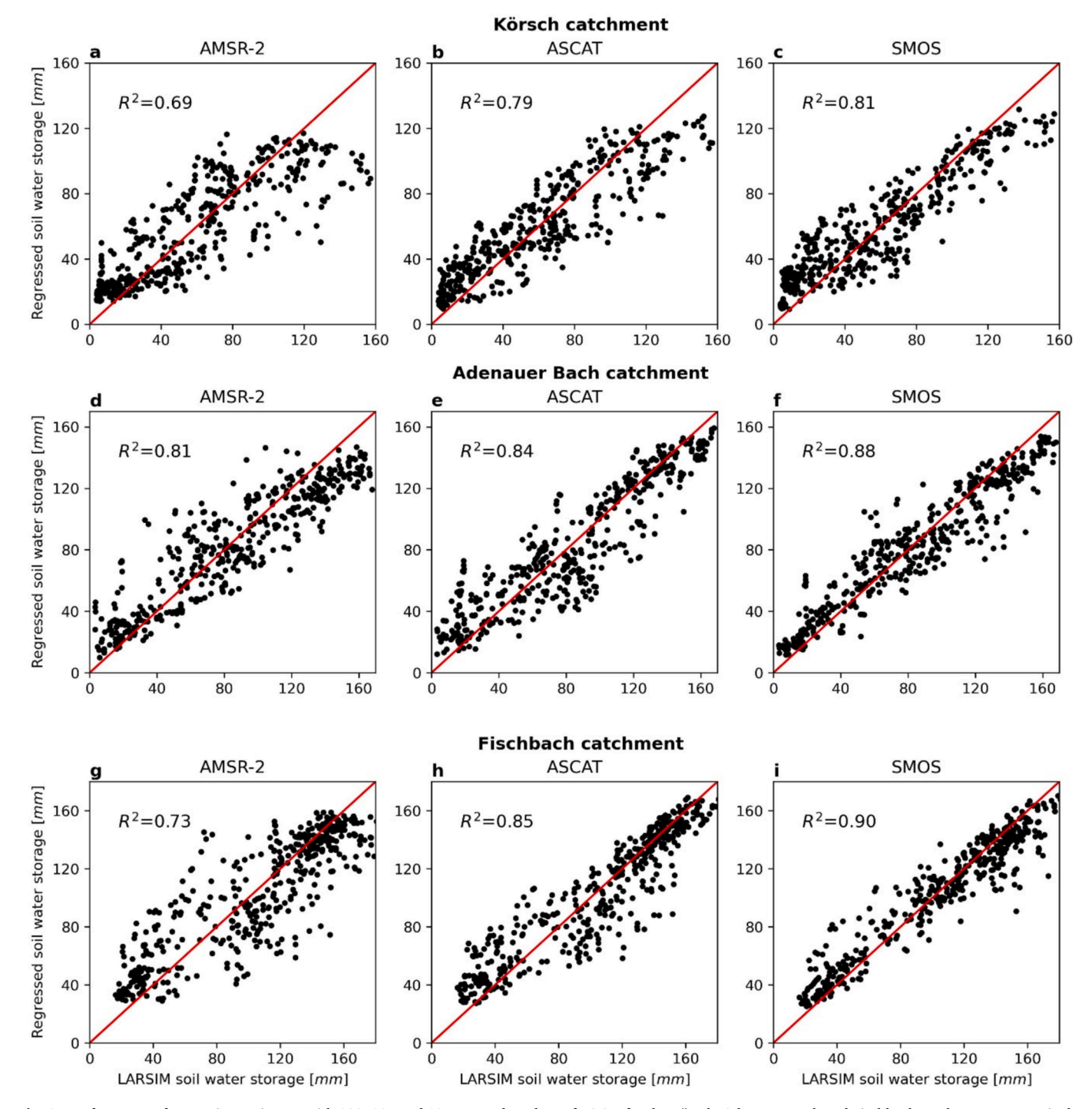


Fig. 9. Performance of regressions using RF with 120, 105 and 105 antecedent days of RS SM for the Körsch, Adenauer Bach and Fischbach catchments, respectively. Three RS SM products were used, i.e. AMSR-2 (a, d and g), ASCAT (b, e and h) and SMOS (c, f and i).

mountainous Adenauer Bach and Fischbach catchments in Germany, representing two different types of catchments prone to flash floods. Considering antecedent RS SM can result in good relationships between RS SM and model soil water storage for the three studied catchments since antecedent RS SM can to some extent provide SM information of present deeper soil layers. Assimilating the inferred soil water storage in the coupled LARSIM-PDAF model can enhance flood modeling in terms of the general performance (increase of  $\sim 0.22$  in KGE), flood peak errors (reduction of  $\sim 15$ % in the mean error), and uncertainty reduction in soil wetness simulations. The approach can be transferred to other RS products, such as ASCAT and SMOS. Although proper assimilation of RS

SM can improve flash flood simulations, it is observed that uncertainty in precipitation has a very large impact on simulating flash floods. Therefore, reducing, or better quantifying precipitation uncertainty will always be important for flash flood modeling in the future. Due to the availability of SMAP SM since 2015, we tested our new approach for four events per catchment. Future work should find more catchments affected by flash floods and more events to better verify the performance of the proposed approach. Nevertheless, the proposed approach considering the antecedent RS SM in the coupled flash flood and data assimilation model provides a feasible way to appropriately use RS SM for data assimilation for hydrological models with few or even a single

soil laver.

# CRediT authorship contribution statement

Yan Liu: Writing – review & editing, Writing – original draft, Visualization, Validation, Methodology, Formal analysis, Conceptualization. Yong Chang: Writing – review & editing, Methodology. Ingo Haag: Writing – review & editing, Methodology. Julia Krumm: Writing – review & editing, Methodology. Visakh Sivaprasad: Writing – review & editing, Methodology. Dirk Aigner: Writing – review & editing, Methodology. Harry Vereecken: Writing – review & editing, Supervision. Harrie-Jan Hendricks Franssen: Writing – review & editing, Supervision, Methodology, Funding acquisition, Conceptualization.

# Declaration of competing interest

The authors declare that they have no known competing financial interests or personal relationships that could have appeared to influence the work reported in this paper.

# Acknowledgements

This research was supported by the AVOSS project (No.: DB002082) funded by BMBF (German Federal Ministry of Education and Research). We thank colleagues from the AVOSS project for discussion, particularly Markus Weiler and Andreas Hänsler for the selection of study sites. We also thank Lars Nerger for the discussion about PDAF settings in our research. We acknowledge Landesanstalt für Umwelt Baden-Württemberg (LUBW) and Landesamt für Umwelt Rheinland-Pfalz (LfU) for the agreement of using their LARSIM models for Körsch, Adenauer Bach, and Fischbach, respectively, and providing hourly streamflow observations. Open Access funding was organized by Projekt DEAL.

# Appendix A. Supplementary data

Supplementary data to this article can be found online at https://doi.org/10.1016/j.jhydrol.2024.132395.

# Data availability

Data will be made available on request.

# References

- Abdulraheem, M.I., Zhang, W., Li, S., Moshayedi, A.J., Farooque, A.A., Hu, J., 2023. Advancement of Remote Sensing for Soil Measurements and Applications: A Comprehensive Review. Sustainability 15, 15444.
- Arabameri, A., Saha, S., Chen, W., Roy, J., Pradhan, B., Bui, D.T., 2020. Flash flood susceptibility modelling using functional tree and hybrid ensemble techniques. J Hydrol (amst) 587. https://doi.org/10.1016/j.jhydrol.2020.125007.
- Bárdossy, A., Kilsby, C., Birkinshaw, S., Wang, N., Anwar, F., 2022. Is Precipitation Responsible for the Most Hydrological Model Uncertainty? Frontiers in Water 4. https://doi.org/10.3389/frwa.2022.836554.
- Bartalis, Z., Wagner, W., Naeimi, V., Hasenauer, S., Scipal, K., Bonekamp, H., Figa, J., Anderson, C., 2007. Initial soil moisture retrievals from the METOP-A advanced Scatterometer (ASCAT). Geophys. Res. Lett. 34, L20401. https://doi.org/10.1029/ 2007GL031088.
- Beven, K., 1993. Prophecy, reality and uncertainty in distributed hydrological modelling.

  Adv Water Resour 16, 41–51. https://doi.org/10.1016/0309-1708(93)90028-E.

  Beven, K. 2012. Rainfall-Runoff Modelling The Primer 2nd Edition. Wiley Blackwell
- Beven, K., 2012. Rainfall-Runoff Modelling The Primer, 2nd Edition,. Wiley Blackwell, p. 457.
- Breiman, L., 2001. Random Forests. Machine Learning 45, 5–32.
- Bremicker, M., 2000. Das Wasserhaushaltsmodell LARSIM. Modellgrundlagen und Anwendungsbeispiele, Freiburger Schriften zur Hydrologie, p. 11.
- Bremicker, M., Brahmer, G., Demuth, N., Holle, F.-K., Haag, I., 2013. Räumlich hoch aufgelöste LARSIM Wasserhaushaltsmodelle für die Hochwasservorhersage und weitere Anwendung. KW Korrespondenz Wasserwirtschaft 6 (9), 509–519.
- Butts, M.B., Payne, J.T., Kristensen, M., Madsen, H., 2004. An evaluation of the impact of model structure on hydrological modelling uncertainty for streamflow simulation. Journal of Hydrology. 242–266. https://doi.org/10.1016/j.jhydrol.2004.03.042.
- Cenci, L., Pulvirenti, L., Boni, G., Chini, M., Matgen, P., Gabellani, S., Squicciarino, G., Pierdicca, N., 2017. An evaluation of the potential of Sentinel 1 for improving flash

- flood predictions via soil moisture-data assimilation. Advances in Geosciences 44, 89–100. https://doi.org/10.5194/adgeo-44-89-2017.
- Chan, S.K., Bindlish, R., O'Neill, P., Jackson, T., Njoku, E., Dunbar, S., Chaubell, J., Piepmeier, J., Yueh, S., Entekhabi, D., 2018. Development and assessment of the SMAP enhanced passive soil moisture product. Remote Sens Environ 204, 931–941.
- Chang, Y., Liu, Y., Liu, L., 2023. Contrasting hydrological responses to climate change in two adjacent catchments dominated by karst and nonkarst. J Hydrol (amst) 625. https://doi.org/10.1016/j.jhydrol.2023.130013.
- Chollet, F., and Others, 2015. Keras. GitHub repository. https://github.com/keras-team/keras.
- Corral, C., Berenguer, M., Sempere-Torres, D., Poletti, L., Silvestro, F., Rebora, N., 2019. Comparison of two early warning systems for regional flash flood hazard forecasting. J Hydrol (amst) 572, 603–619. https://doi.org/10.1016/j.jhydrol.2019.03.026.
- Crow, W.T., Chen, F., Reichle, R.H., Liu, Q., 2017. L band microwave remote sensing and land data assimilation improve the representation of prestorm soil moisture conditions for hydrologic forecasting. Geophys Res Lett 44, 5495–5503. https://doi.org/10.1002/2017GL073642.
- Crow, W.T., Ryu, D., 2009. Hydrology and Earth System Sciences A new data assimilation approach for improving runoff prediction using remotely-sensed soil moisture retrievals. Hydrol. Earth Syst, Sci.
- Crow, W.T., Van Den Berg, M.J., Huffman, G.J., Pellarin, T., 2011. Correcting rainfall using satellite-based surface soil moisture retrievals: The Soil Moisture Analysis Rainfall Tool (SMART). Water Resour Res 47. https://doi.org/10.1029/ 2011WR010576.
- De Lannoy, G.J.M., Reichle, R.H., 2016. Global assimilation of multiangle and multipolarization SMOS brightness temperature observations into the GEOS-5 catchment land surface model for soil moisture estimation. J Hydrometeorol 17, 669–691. https://doi.org/10.1175/JHM-D-15-0037.1.
- De Santis, D., Biondi, D., Crow, W.T., Camici, S., Modanesi, S., Brocca, L., Massari, C., 2021. Assimilation of satellite soil moisture products for river flow prediction: An extensive experiment in over 700 catchments throughout europe. Water Resour Res 57. https://doi.org/10.1029/2021WR029643.
- Desai, S., Ouarda, T.B.M.J., 2021. Regional hydrological frequency analysis at ungauged sites with random forest regression. J Hydrol (amst) 594. https://doi.org/10.1016/j. jhydrol.2020.125861.
- Douinot, A., Roux, H., Garambois, P.-A., Larnier, K., Labat, D., Dartus, D., 2016. Accounting for rainfall systematic spatial variability in flash flood forecasting. J Hydrol (amst) 541, 359–370.
- Dunne, T., Zhang, W., Aubry, B.F., 1991. Effects of rainfall, vegetation, and microtopography on infiltration and runoff. Water Resour Res 27, 2271–2285.
- El Hajj, M., Baghdadi, N., Zribi, M., Rodríguez-Fernández, N., Wigneron, J.P., Al-Yaari, A., Al Bitar, A., Albergel, C., Calvet, J.-C., 2018. Evaluation of SMOS, SMAP, ASCAT and Sentinel-1 soil moisture products at sites in Southwestern France. Remote Sens (basel) 10, 569.
- Entekhabi, D., Njoku, E.G., O'Neill, P.E., Kellogg, K.H., Crow, W.T., Edelstein, W.N., Entin, J.K., Goodman, S.D., Jackson, T.J., Johnson, J., Kimball, J., Piepmeier, J.R., Koster, R.D., Martin, N., McDonald, K.C., Moghaddam, M., Moran, S., Reichle, R., Shi, J.C., Spencer, M.W., Thurman, S.W., Tsang, L., Van Zyl, J., 2010. The soil moisture active passive (SMAP) mission. Proceedings of the IEEE 98, 704–716. https://doi.org/10.1109/JPROC.2010.2043918.
- Evensen, G., 1994. Sequential data assimilation with a nonlinear quasi-geostrophic model using Monte Carlo methods to forecast error statistics. J Geophys Res Oceans 99, 10143–10162.
- Flamig, Z.L.Z.L., Vergara, H., Gourley, J.J., 2020. The Ensemble Framework for Flash Flood Forecasting (EF5) v1.2: Description and case study. Geosci Model Dev 13, 4943–4958. https://doi.org/10.5194/gmd-13-4943-2020.
- Fowler, H.J., Lenderink, G., Prein, A.F., Westra, S., Allan, R.P., Ban, N., Barbero, R., Berg, P., Blenkinsop, S., Do, H.X., Guerreiro, S., Haerter, J.O., Kendon, E.J., Lewis, E., Schaer, C., Sharma, A., Villarini, G., Wasko, C., Zhang, X., 2021. Anthropogenic intensification of short-duration rainfall extremes. Nat Rev Earth Environ. https://doi.org/10.1038/s43017-020-00128-6.
- Guerreiro, S.B., Fowler, H.J., Barbero, R., Westra, S., Lenderink, G., Blenkinsop, S., Lewis, E., Li, X.F., 2018. Detection of continental-scale intensification of hourly rainfall extremes. Nat Clim Chang. https://doi.org/10.1038/s41558-018-0245-3.
- Gupta, H.V., Kling, H., Yilmaz, K.K., Martinez, G.F., 2009. Decomposition of the mean squared error and NSE performance criteria: Implications for improving hydrological modelling. J Hydrol (amst) 377, 80–91. https://doi.org/10.1016/j. ihydrol.2009.08.003.
- Haag, I., Johst, M., Sieber, A., Bremicker M., 2020. Leitfaden zur Kalibrierung von LARSIM-Wasserhaushaltsmodellen für den operationellen Einsatz in der Hochwasservorhersage. 2. Auflage, LARSIM-Entwicklergemeinschaft.
- Haag, I., Krumm, J., Aigner, D., Steinbrich, A., Weiler, M., 2022. Simulation von Hochwasserereignissen in Folge lokaler Starkregen mit dem Wasserhaushaltsmodell LARSIM. Hydrologie & Wasserbewirtschaftung 66 (1), 6–27. https://doi.org/ 10.5675/HyWa 2022.1 1.
- Han, X., Franssen, H.J.H., Montzka, C., Vereecken, H., 2014. Soil moisture and soil properties estimation in the Community Land Model with synthetic brightness temperature observations. Water Resour Res 50, 6081–6105. https://doi.org/ 10.1002/2013WR014586.
- Han, E., Merwade, V., Heathman, G.C., 2012. Implementation of surface soil moisture data assimilation with watershed scale distributed hydrological model. J Hydrol (amst) 416–417, 98–117. https://doi.org/10.1016/j.jhydrol.2011.11.039.
- Hapuarachchi, H.A.P., Wang, Q.J., Pagano, T.C., 2011. A review of advances in flash flood forecasting. Hydrol Process 25, 2771–2784. https://doi.org/10.1002/ hyp.8040.

- Hartmann, A., Barberá, J.A., Lange, J., Andreo, B., Weiler, M., 2013. Progress in the hydrologic simulation of time variant recharge areas of karst systems – Exemplified at a karst spring in Southern Spain. Adv Water Resour 54, 149–160. https://doi.org/ 10.1016/j.advwatres.2013.01.010.
- Hochreiter, S., Schmidhuber, J., 1997. Long Short-Term Memory. Neural Comput 9, 1735–1780. https://doi.org/10.1162/neco.1997.9.8.1735.
- Houser, P.R., Shuttleworth, W.J., Famiglietti, J.S., Gupta, H.V., Syed, K.H., Goodrich, D. C., 1998. Integration of soil moisture remote sensing and hydrologic modeling using data assimilation. Water Resour Res 34, 3405–3420. https://doi.org/10.1029/1998WR900001
- Kavetski, D., Kuczera, G., Franks, S.W., 2006a. Bayesian analysis of input uncertainty in hydrological modeling: 1. Theory. Water Resour Res 42. https://doi.org/10.1029/ 2005WR004368.
- Kavetski, D., Kuczera, G., Franks, S.W., 2006b. Bayesian analysis of input uncertainty in hydrological modeling: 2. Application. Water Resour Res 42. https://doi.org/ 10.1029/2005WR004376
- Kerr, Y.H., Font, J., Martin-Neira, M., Mecklenburg, S., 2012. Introduction to the special issue on the ESA's Soil Moisture and Ocean Salinity Mission (SMOS): instrument performance and first results. IEEE Transactions on Geoscience and Remote Sensing 50, 1351–1353.
- Kratzert, F., Klotz, D., Brenner, C., Schulz, K., Herrnegger, M., 2018. Rainfall-runoff modelling using Long Short-Term Memory (LSTM) networks. Hydrol Earth Syst Sci 22, 6005–6022. https://doi.org/10.5194/hess-22-6005-2018.
- Laio, F., Di Baldassarre, G., Montanari, A., 2009. Model selection techniques for the frequency analysis of hydrological extremes. Water Resour Res 45. https://doi.org/ 10.1029/2007WR006666.
- Laiolo, P., Gabellani, S., Campo, L., Silvestro, F., Delogu, F., Rudari, R., Pulvirenti, L., Boni, G., Fascetti, F., Pierdicca, N., Crapolicchio, R., Hasenauer, S., Puca, S., 2016. Impact of different satellite soil moisture products on the predictions of a continuous distributed hydrological model. International Journal of Applied Earth Observation and Geoinformation 48, 131–145. https://doi.org/10.1016/j.jag.2015.06.002.
- LEG LARSIM Entwicklergemeinschaft (2023): Das Wasserhaushaltsmodell LARSIM Modellgrundlagen und Anwendungsbeispiele. http://www.larsim.info/dokumentation/LARSIM-Dokumentation.pdf, Stand: 06.04.2023.
- Li, Y., Ryu, D., Western, A.W., Wang, Q.J., 2015. Assimilation of stream discharge for flood forecasting: Updating a semidistributed model with an integrated data assimilation scheme. Water Resour Res 51, 3238–3258. https://doi.org/10.1002/ 2014WR016667.
- Li, X., Wigneron, J.-P., Fan, L., Frappart, F., Yueh, S.H., Colliander, A., Ebtehaj, A., Gao, L., Fernandez-Moran, R., Liu, X., 2022. A new SMAP soil moisture and vegetation optical depth product (SMAP-IB): Algorithm, assessment and intercomparison. Remote Sens Environ 271, 112921.
- Lievens, H., De Lannoy, G.J.M., Al Bitar, A., Drusch, M., Dumedah, G., Hendricks Franssen, H.J., Kerr, Y.H., Tomer, S.K., Martens, B., Merlin, O., Pan, M., Roundy, J. K., Vereecken, H., Walker, J.P., Wood, E.F., Verhoest, N.E.C., Pauwels, V.R.N., 2016. Assimilation of SMOS soil moisture and brightness temperature products into a land surface model. Remote Sens Environ 180, 292–304. https://doi.org/10.1016/j. rse.2015.10.033.
- Lindström, G., Johansson, B., Persson, M., Gardelin, M., Bergström, S., 1997.
  Development and test of the distributed HBV-96 hydrological model, Journal of Hydrology, FLSEVIER. Journal of Hydrology.
- Liu, Y., Wagener, T., Beck, H.E., Hartmann, A., 2020. What is the hydrologically effective area of a catchment? Environmental Research Letters 15. https://doi.org/10.1088/ 1748-9326/aba7e5.
- Liu, Y., Fernández-Ortega, J., Mudarra, M., Hartmann, A., 2022. Pitfalls and a feasible solution for using KGE as an informal likelihood function in MCMC methods: DREAM(ZS) as an example. Hydrol Earth Syst Sci 26, 5341–5355. https://doi.org/ 10.5194/hess-26-5341-2022.
- López López, P., Wanders, N., Schellekens, J., Renzullo, L.J., Sutanudjaja, E.H., Bierkens, M.F.P., 2016. Improved large-scale hydrological modelling through the assimilation of streamflow and downscaled satellite soil moisture observations. Hydrol Earth Syst Sci 20, 3059–3076. https://doi.org/10.5194/hess-20-3059-2016.
- Ma, M., Zhao, G., He, B., Li, Q., Dong, H., Wang, S., Wang, Z., 2021. XGBoost-based method for flash flood risk assessment. J Hydrol (amst) 598. https://doi.org/ 10.1016/j.jhydrol.2021.126382.
- Mahdi El Khalki, E., Tramblay, Y., Massari, C., Brocca, L., Simonneaux, V., Gascoin, S., El Mehdi Saidi, M., 2020. Challenges in flood modeling over data-scarce regions: How to exploit globally available soil moisture products to estimate antecedent soil wetness conditions in Morocco. Natural Hazards and Earth System Sciences 20, 2591–2607. https://doi.org/10.5194/nhess-20-2591-2020.
- Naz, B.S., Kurtz, W., Montzka, C., Sharples, W., Goergen, K., Keune, J., Gao, H., Springer, A., Franssen, H.J.H., Kollet, S., 2019. Improving soil moisture and runoff simulations at 3&km over Europe using land surface data assimilation. Hydrol Earth Syst Sci 23, 277–301. https://doi.org/10.5194/hess-23-277-2019.
- NERGER, L., HILLER, W., SCHRÖTER, J., 2005. PDAF THE PARALLEL DATA ASSIMILATION FRAMEWORK: EXPERIENCES WITH KALMAN FILTERING, in: Use of High Performance Computing in Meteorology. WORLD SCIENTIFIC, pp. 63–83. https://doi.org/doi:10.1142/9789812701831\_0006.

- Nikolopoulos, E.I., Anagnostou, E.N., Borga, M., Vivoni, E.R., Papadopoulos, A., 2011. Sensitivity of a mountain basin flash flood to initial wetness condition and rainfall variability. J Hydrol (amst) 402, 165–178. https://doi.org/10.1016/j.ibydrol.2010.12.020
- Oliva, R., Martin-Neira, M., Corbella, I., Torres, F., Kainulainen, J., Tenerelli, J.E., Cabot, F., Martin-Porqueras, F., 2012. SMOS calibration and instrument performance after one year in orbit. IEEE Transactions on Geoscience and Remote Sensing 51, 654-670.
- Parinussa, R.M., Holmes, T.R.H., Wanders, N., Dorigo, W.A., de Jeu, R.A.M., 2015. A Preliminary Study toward Consistent Soil Moisture from AMSR2. J. Hydrometeor. 16, 932–947. https://doi.org/10.1175/JHM-D-13-0200.1.
- Pauwels, V.R.N., Hoeben, R., Verhoest, N.E.C., De Troch, F.P., 2001. The importance of the spatial patterns of remotely sensed soil moisture in the improvement of discharge predictions for small-scale basins through data assimilation. J Hydrol (amst) 251, 88-102. https://doi.org/10.1016/S0022-1694(01)00440-1.
- Pauwels, V.R.N., Hendricks Franssen, H.J., de Lannoy, G.J.M., 2020. Evaluation of State and Bias Estimates for Assimilation of SMOS Retrievals into Conceptual Rainfall-Runoff Models. Frontiers in Water 2, 4. https://doi.org/10.3389/frwa.2020.00004.
- Pedregosa, F., Varoquaux, G., Gramfort, A., Michel, V., Thirion, B., Grisel, O., Blondel, M., Prettenhofer, P., Weiss, R., Dubourg, V., 2011. Scikit-learn: Machine learning in Python. The Journal of Machine Learning Research 12, 2825–2830.
- Pianosi, F., Wagener, T., 2016. Understanding the time-varying importance of different uncertainty sources in hydrological modelling using global sensitivity analysis. Hydrol Process 30, 3991–4003. https://doi.org/10.1002/hyp.10968.
- Quintero, F., Sempere-Torres, D., Berenguer, M., Baltas, E., 2012. A scenario-incorporating analysis of the propagation of uncertainty to flash flood simulations. J Hydrol (amst) 460–461, 90–102. https://doi.org/10.1016/j.jhydrol.2012.06.045.
- Saharia, M., Kirstetter, P.E., Vergara, H., Gourley, J.J., Hong, Y., Giroud, M., 2017. Mapping flash flood severity in the united states. J Hydrometeorol 18, 397–411. https://doi.org/10.1175/JHM-D-16-0082.1.
- Thomas Steven Savage, J., Pianosi, F., Bates, P., Freer, J., Wagener, T., 2016. Quantifying the importance of spatial resolution and other factors through global sensitivity analysis of a flood inundation model. Water Resour Res 52, 9146–9163. https://doi.org/10.1002/2015WR018198.
- Schalla, J., Hartmann, A., Abraham, T., Liu, Y., 2023. Global hydrological parameter estimates to local applications: Influence of forcing and catchment properties. Hydrology Research 54, 475–490. https://doi.org/10.2166/NH.2023.086.
- Schoups, G., Vrugt, J.A., 2010. A formal likelihood function for parameter and predictive inference of hydrologic models with correlated, heteroscedastic, and non-Gaussian errors. Water Resour Res 46. https://doi.org/10.1029/2009WR008933.
- Steinbrich, A., Leistert, H., Weiler, M., 2016. Model-based quantification of runoff generation processes at high spatial and temporal resolution. Environ Earth Sci 75. https://doi.org/10.1007/s12665-016-6234-9.
- Strebel, L., Bogena, H.R., Vereecken, H., Hendricks Franssen, H.J., 2022. Coupling the Community Land Model version 5.0 to the parallel data assimilation framework PDAF: Description and applications. Geosci Model Dev 15, 395–411. https://doi. org/10.5194/gmd-15-395-2022.
- Thompson, S.E., Harman, C.J., Heine, P., Katul, G.G., 2010. Vegetation-infiltration relationships across climatic and soil type gradients. J Geophys Res Biogeosci 115.
- Tramblay, Y., Bouaicha, R., Brocca, L., Dorigo, W., Bouvier, C., Camici, S., Servat, E., 2012. Estimation of antecedent wetness conditions for flood modelling in northern Morocco. Hydrol Earth Syst Sci 16, 4375–4386. https://doi.org/10.5194/hess-16-4375-2012
- Wagener, T., Boyle, D.P., Lees, M.J., Wheater, H.S., Gupta, H.V., Sorooshian, S., 2001.

  A framework for development and application of hydrological models A framework for development and application of hydrological models. Hydrology and Earth System Sciences.
- Wagner, W., Lemoine, G., Borgeaud, M., Rott, H., 1999. A study of vegetation cover effects on ERS scatterometer data. IEEE Transactions on Geoscience and Remote Sensing 37, 938–948.
- Westra, S., Fowler, H.J., Evans, J.P., Alexander, L.V., Berg, P., Johnson, F., Kendon, E.J., Lenderink, G., Roberts, N.M., 2014. Future changes to the intensity and frequency of short-duration extreme rainfall. Reviews of Geophysics. https://doi.org/10.1002/ 201486.000464
- Yatheendradas, S., Wagener, T., Gupta, H., Unkrich, C., Goodrich, D., Schaffner, M., Stewart, A., 2008. Understanding uncertainty in distributed flash flood forecasting for semiarid regions. Water Resour Res 44.
- Zhai, X., Zhang, Y., Zhang, Y., Guo, L., Liu, R., 2021. Simulating flash flood hydrographs and behavior metrics across China: Implications for flash flood management. Science of the Total Environment 763. https://doi.org/10.1016/j.scitotenv.2020.142977.
- Zhang, Y., Chiew, F.H.S., Li, M., Post, D., 2018. Predicting Runoff Signatures Using Regression and Hydrological Modeling Approaches. Water Resour Res 54, 7859–7878. https://doi.org/10.1029/2018WR023325.
- Zhao, G., Liu, R., Yang, M., Tu, T., Ma, M., Hong, Y., Wang, X., 2022. Large-scale flash flood warning in China using deep learning. J Hydrol (amst) 604. https://doi.org/ 10.1016/j.jhydrol.2021.127222.